

Di- and Trinuclear Polyhydride Complexes Containing Ruthenium and Rhenium. Synthesis, Site Exchange, and H/D Exchange of Hydride Ligands†

Jun-ichi Ito, Takanori Shima, and Hiroharu Suzuki*

Department of Applied Chemistry, Graduate School of Science and Engineering,
Tokyo Institute of Technology and CREST, Japan Science and Technology Corporation (JST),
O-okayama, Meguro-ku, Tokyo 152-8552, Japan

Received November 3, 2003

Novel di- and trinuclear heterometallic polyhydride complexes containing both ruthenium and rhenium atoms have been synthesized. Treatment of $(\text{Cp}'\text{RuH}_2)_2$ (**1**) with $\text{Cp}'\text{ReH}_6$ affords the heterobimetallic polyhydride complex $\text{Cp}'\text{Ru}(\mu\text{-H})_3\text{ReH}_2\text{Cp}'$ (**6**) together with the corresponding two heterotrimetallic polyhydride complexes $(\text{Cp}'\text{Ru})_2(\text{Cp}'\text{Re})(\mu\text{-H})_4$ (**7**) and $(\text{Cp}'\text{Ru})(\text{Cp}'\text{Re})_2(\text{H})_5$ (**8**). These new polyhydride complexes have notably only C_5Me_5 groups as auxiliary ligands. A new class of a dinuclear polyhydride complex, $\text{Cp}'\text{Ru}(\mu\text{-H})_3\text{ReH}(\text{triphos})$ (**9**), which has a different kind of auxiliary ligand on each of the metal centers, has been prepared by the reaction of $(\text{triphos})\text{ReH}_5$ (**4**; triphos = $\text{CH}_3\text{C}(\text{CH}_2\text{PPh}_2)_3$) with $(\text{Cp}'\text{RuOme})_2$ (**5**). The trinuclear polyhydride **7** is alternatively synthesized by way of an intermediary cationic complex, $[(\text{Cp}'\text{Ru})_2(\text{Cp}'\text{Re})(\mu\text{-H})_5][\text{BF}_4]$ (**10a**), obtained by treatment of **6** with HBF_4 . Treatment of $(\text{Cp}'\text{ReH}_3)_2$ (**3**) with **5** results in the formation of the trimetallic complex **8** with a triangular Re_2Ru framework. The X-ray diffraction studies have proved the bimetallic structures of **6** and **9**, which have both terminal and bridging hydrides. The hydride ligands coordinated in both **6** and **9** exchange coordination sites, and the exchange process has been analyzed by means of NMR spectroscopy. The molecular structures of trinuclear clusters **7'** and **10b'** have been determined by X-ray diffraction studies. The trinuclear complexes **7**, **8**, and **10** undergo an H/D exchange reaction between the hydride ligands and atmospheric D_2 . The H/D exchange reaction of hydride in complexes **7** and **8** with C_6D_6 is a slow process, because of the bulkiness of the C_6D_6 molecule relative to the size of the reaction field surrounded by the three Cp' groups.

Introduction

We have thus far reported the synthesis of a series of a new class of polyhydride cluster complexes of ruthenium, $\{(\eta^5\text{-C}_5\text{R}_5)\text{Ru}\}_n(\text{H})_{n+2}$ ($\text{C}_5\text{R}_5 = \text{C}_5\text{H}_5, \text{C}_5\text{Me}_5, \text{C}_5\text{MeH}_4, \text{C}_5\text{Me}_2\text{H}_3$; $n = 2\text{--}5$), and demonstrated that they activated various hydrocarbons, including alkanes, in an unprecedented fashion due to cooperative action of the metal centers.¹ We have also synthesized a highly reactive iron analogue of a diruthenium tetrahydride cluster.²

In contrast to a homonuclear metal cluster complex, composed of the same kind of metals, a heterometallic cluster has an electronically anisotropic reaction field resulting from polarization of the metal–metal bond. It is, therefore, anticipated that the metal centers play

mutually different roles, namely, a binding site and an activation site, in such heterometallic clusters.

Although several examples of heteronuclear polyhydride clusters have been reported,^{3,4} there is no precedent of having only the C_5Me_5 group as an auxiliary ligand. We have recently achieved the synthesis of the heterobimetallic polyhydride complexes $\text{Cp}'\text{Ru}(\mu\text{-H})_3\text{IrCp}'$ and $\text{Cp}'\text{Ru}(\mu\text{-H})_3\text{MH}_3\text{Cp}'$ ($\text{M} = \text{Mo}, \text{W}$).⁵ As anticipated, remarkable site selectivity at the metal centers was observed in the reaction of $\text{Cp}'\text{Ru}(\mu\text{-H})_3\text{IrCp}'$ with ethylene. The ruthenium center takes the part of a binding

* To whom correspondence should be addressed.

† Dedicated with admiration and appreciation to Professor Akio Yamamoto and Dr. Nobuhiro Tamura, technical director of the CREST project.

(1) (a) Suzuki, H.; Omori, H.; Lee, D. H.; Yoshida, Y.; Fukushima, M.; Tanaka, M.; Moro-oka, Y. *Organometallics* **1994**, *13*, 1129. (b) Matsubara, K.; Inagaki, A.; Tanaka, M.; Suzuki, H. *J. Am. Chem. Soc.* **1999**, *121*, 7421. (c) Ohki, Y.; Suzuki, H. *Angew. Chem., Int. Ed.* **2000**, *39*, 3463. (d) Inagaki, A.; Takemori, T.; Tanaka, M.; Suzuki, H. *Angew. Chem., Int. Ed.* **2000**, *39*, 404. (e) Takemori, T.; Inagaki, A.; Suzuki, H. *J. Am. Chem. Soc.* **2001**, *123*, 1762. (f) Ohki, Y.; Uehara, N.; Suzuki, H. *Angew. Chem., Int. Ed.* **2002**, *41*, 4085. (g) Ohki, Y.; Uehara, N.; Suzuki, H. *Organometallics* **2003**, *22*, 59.

(2) Ohki, Y.; Suzuki, H. *Angew. Chem., Int. Ed.* **2000**, *39*, 3120.

(3) (a) Moldes, I.; Delavaux-Nicot, B.; Lugan, N.; Mathieu, R. *Inorg. Chem.* **1994**, *33*, 3510. (b) Alvarez, D.; Caulton, K. G.; Evans, W. J.; Ziller, J. W. *Inorg. Chem.* **1992**, *31*, 5500. (c) Sluys, L. S. V. D.; Miller, M. M.; Kubas, G. J.; Caulton, K. G. *J. Am. Chem. Soc.* **1991**, *113*, 2513. (d) Alvarez, D.; Lundquist, E. G.; Ziller, J. W.; Evans, W. J.; Caulton, K. G. *J. Am. Chem. Soc.* **1989**, *111*, 8392. (e) Musco, A.; Naegeli, R.; Venanzi, L. M. *J. Organomet. Chem.* **1982**, *228*, C15. (f) Poulton, J. T.; Folting, K.; Caulton, K. G. *Organometallics* **1992**, *11*, 1364. (g) Batsanov, A. D.; Howard, J. A. K.; Love, J. B.; Spencer, J. L. *Organometallics* **1995**, *14*, 5657. (h) Alvarez, D.; Caulton, K. G.; Evans, W. J.; Ziller, J. W. *J. Am. Chem. Soc.* **1990**, *112*, 5674. (i) Geerts, R. L.; Huffman, J. C.; Caulton, K. G. *Inorg. Chem.* **1986**, *25*, 590. (j) Weng, W.; Arif, A. M.; Ernst, R. D. *J. Cluster Sci.* **1996**, *7*, 629. (k) Bakmutov, I. V.; Vorontsov, E. V.; Boni, G.; Moise, C. *Inorg. Chem.* **1997**, *36*, 4055. (l) Dranbins, M. H.; Bau, R.; Mason, S. A.; Freeman, J. W.; Ernst, R. D. *Eur. J. Inorg. Chem.* **1998**, 851.

(4) (a) He, Z.; Plasseraud, L.; Moldes, I.; Dahan, F.; Neibecker, D.; Etienne, M.; Mathieu, R. *Angew. Chem., Int. Ed. Engl.* **1995**, *34*, 916. (b) Moldes, I.; Nefedov, S.; Lugan, N.; Mathieu, R. *J. Organomet. Chem.* **1995**, *490*, 11. (c) He, Z.; Nefedov, S.; Lugan, N.; Neibecker, D.; Mathieu, R. *Organometallics* **1993**, *12*, 3837. (d) He, Z.; Neibecker, D.; Lugan, N.; Mathieu, R. *Organometallics* **1992**, *11*, 817.

site, and the iridium center, in turn, plays the role of an activation site. In the reaction of the Ru–Mo or Ru–W clusters with two-electron-donor ligands such as amine and phosphine, the donor ligand exclusively attacks the group VI metal site.

The reactivity of a heteronuclear cluster complex is strongly affected by the combination of the metals that compose the cluster, as well as the supporting ligands. As an extension of the chemistry of the heteronuclear cluster, we have synthesized a new class of clusters containing ruthenium and group VII metals. The rhenium atom often has a high oxidation state and coordination number, in contrast to a late transition metal such as iridium,⁶ which has been combined with ruthenium as a component of the heterobimetallic cluster. Therefore, the combination of rhenium and ruthenium in the heteronuclear cluster probably enhances the anisotropy of the reaction field.

All of the Ru–Re heterobimetallic polyhydride complexes reported thus far have CO as the auxiliary ligand.⁴ Although they are useful and important in the catalytic reaction in which carbon monoxide is involved, they are usually less active in oxidative addition because of a decrease in electron density at the metal centers due to coordination of strongly electron-withdrawing carbon monoxide. In contrast, electron density at the metal centers in the metal hydride cluster is most certainly higher than in the metal–carbonyl cluster. Therefore, we expected that the metal polyhydride cluster was much more active than the metal–carbonyl cluster in the oxidative addition of substrates.

Another interesting aspect of the polyhydride cluster is the relation between the mobility of the hydride ligands and the reactivity. Recently, we reported that site exchange of hydride ligands in the silylene complex $(\text{Cp}'\text{Ru})_2(\mu\text{-SiR}_2)_2(\mu\text{-H})_2$ proceeded via an intermediary $\mu\text{-SiR}_2\text{H}$ complex, and as a result, a vacant site was generated at one of the two ruthenium centers.⁷ Site exchange of the hydride ligands via an intermediary $\eta^2\text{-H}_2$ complex is also proposed for the polyhydride complex.⁸ If site exchange of hydrides in the polyhydride cluster also proceeds via an $\eta^2\text{-H}_2$ complex, a vacant coordination site should be formed during the reaction. Thus, the mobility of hydride ligands, especially the capability of hydrides to exchange the coordination site, would be closely connected with the ease of forming the vacant site. Analysis of the dynamic process of the hydride is, therefore, helpful for a better understanding of the reactivity of the polyhydride cluster.

We report herein the synthesis of novel di- and

trinuclear heterometallic polyhydride clusters containing ruthenium and rhenium which have no auxiliary ligands other than Cp' and triphos (triphos = $\text{CH}_3\text{C}(\text{CH}_2\text{PPh}_2)_3$) ligands. Some reactions with regard to mobility of the hydride ligands, such as site-exchange reactions of the hydrides, are also reported.

Experimental Section

All air- and moisture-sensitive compounds were manipulated using standard Schlenk and vacuum line techniques under an argon atmosphere. Toluene, ether, and tetrahydrofuran were distilled from sodium benzophenone ketyl prior to use. Pentane was dried over P_2O_5 and distilled prior to use. Benzene- d_6 , toluene- d_8 , and tetrahydrofuran- d_8 were distilled from sodium benzophenone ketyl. Other reagents were used as received. The known complexes $(\text{Cp}'\text{RuH}_2)_2$ (**1**),^{1a} $\text{Cp}'\text{ReH}_6$ (**2**),⁹ $(\text{Cp}'\text{ReH}_3)_2$ (**3**),¹⁰ (triphos)ReH₅ (**4**),¹¹ and $(\text{Cp}'\text{RuOMe})_2$ (**5**),¹² and $(\text{Cp}'\text{RuCl})_4$ ¹³ were prepared according to the literature.

¹H, ¹³C, and ³¹P NMR spectra were recorded on a Varian INOVA-400. ¹H NMR spectra were referenced to TMS as an internal standard. ¹³C NMR spectra were referenced to the natural-abundance carbon signal of the solvent employed. ³¹P NMR spectra were referenced to an 85% H_3PO_4 external standard. IR spectra were recorded on a Nicolet Avatar 360 FT-IR. Elemental analyses were recorded on a Perkin-Elmer 2400II.

Cp'Ru($\mu\text{-H}$)₃ReH₂Cp' (6**).** A solution of $\text{Cp}'\text{Ru}(\mu\text{-H})_4\text{RuCp}'$ (250.6 mg, 0.526 mmol) and $\text{Cp}'\text{ReH}_6$ (300.8 mg, 0.919 mmol) in toluene (30 mL) was stirred at 80 °C for 36 h. The solution turned from red to dark brown. Then, the mixture was evaporated to dryness. The residue was extracted with toluene, and the extract was chromatographed on alumina. A red fraction that eluted with toluene/diethyl ether (5/1) was evaporated to dryness to afford complex **6** (273.9 mg, 0.487 mmol, 53%). The C_5EtMe_4 analogue of **6**, $(\text{C}_5\text{EtMe}_4)\text{Ru}(\mu\text{-H})_3\text{ReH}_2\text{Cp}'$ (**6'**), was prepared in a similar manner by using $(\text{C}_5\text{EtMe}_4)\text{Ru}(\mu\text{-H})_4\text{Ru}(\text{C}_5\text{EtMe}_4)$ as the starting material. **6**: ¹H NMR (400 MHz, C_6D_6 , room temperature, δ /ppm) 2.14 (s, 15H, Cp'Re), 1.84 (s, 15H, Cp'Ru), –10.36 (s, 5H, $\mu\text{-H}$ and Re–H); ¹³C NMR (100 MHz, C_6D_6 , room temperature, δ /ppm) 89.5 (s, $\text{C}_5\text{Me}_5\text{Re}$), 82.2 (s, $\text{C}_5\text{Me}_5\text{Ru}$), 13.2 (q, $J_{\text{CH}} = 127.1$ Hz, $\text{C}_5\text{Me}_5\text{Re}$), 12.5 (q, $J_{\text{CH}} = 125.6$ Hz, $\text{C}_5\text{Me}_5\text{Ru}$); IR (ATR, cm^{-1}) 2962, 2902, 2857, 2000 ($\nu_{\text{Re-H}}$), 1990 ($\nu_{\text{Re-H}}$), 1479, 1377, 1262, 1087, 1071, 1030, 819. Anal. Calcd for $\text{C}_{20}\text{H}_{35}\text{RuRe}$: C, 42.64; H, 6.27. Found: C, 42.56; H, 6.07. **6'**: ¹H NMR (400 MHz, C_6D_6 , room temperature, δ /ppm) 2.38 (q, $J_{\text{HH}} = 7.6$ Hz, 2H, $\text{CH}_3\text{CH}_2\text{-}$), 2.14 (s, 15H, Cp'Re), 1.86 (s, 6H, $\text{C}_5\text{Me}_4\text{EtRu}$), 1.85 (s, 6H, $\text{C}_5\text{Me}_4\text{EtRu}$), 1.05 (t, $J_{\text{HH}} = 7.6$ Hz, 3H, $\text{CH}_3\text{CH}_2\text{-}$), –10.33 (br s, 5H, $\mu\text{-H}$ and Re–H); ¹³C NMR (100 MHz, C_6D_6 , room temperature, δ /ppm) 89.6 (s, $\text{C}_5\text{Me}_5\text{Re}$), 88.3 (s, $\text{C}_5\text{Me}_4\text{EtRu}$), 82.5 (s, $\text{C}_5\text{Me}_4\text{EtRu}$), 81.7 (s, $\text{C}_5\text{Me}_4\text{EtRu}$), 20.5 (t, $J_{\text{CH}} = 124.4$ Hz, $\text{CH}_3\text{CH}_2\text{-}$), 15.8 (q, $J_{\text{CH}} = 125.1$ Hz, $\text{CH}_3\text{CH}_2\text{-}$), 13.2 (q, $J_{\text{CH}} = 126.6$ Hz, $\text{C}_5\text{Me}_5\text{Re}$), 12.5 (q, $J_{\text{CH}} = 125.9$ Hz, $\text{C}_5\text{Me}_4\text{EtRu}$), 12.3 (q, $J_{\text{CH}} = 125.6$ Hz, $\text{C}_5\text{Me}_4\text{EtRu}$).

Complex **6** was prepared by an alternative method. To a solution of $\text{Cp}'\text{ReH}_6$ (51.4 mg, 0.157 mmol) in tetrahydrofuran was added a hexane solution of *n*-BuLi (1.58 M, 0.11 mL). The mixture was heated at 50 °C, and then a tetrahydrofuran solution of $(\text{Cp}'\text{RuCl})_4$ (48.5 mg, 0.0446 mmol) was added. After it was heated to 50 °C for 1 h, the mixture was evaporated to

(5) (a) Shima, T.; Suzuki, H. *Organometallics* **2000**, *19*, 2420. (b) Shima, T.; Ito, J.; Suzuki, H. *Organometallics* **2001**, *20*, 10.

(6) Hlatky, G. G.; Crabtree, R. H. *Coord. Chem. Rev.* **1985**, *65*, 1. (7) Takao, T.; Amako, M.; Suzuki, H. *Organometallics* **2003**, *22*, 3855.

(8) (a) Bergamo, M.; Beringhelli, T.; D'Alfonso, G.; Mercandelli, P.; Sironi, A. *J. Am. Chem. Soc.* **2002**, *124*, 5117. (b) Bakmutov, V.; Bürgi, T.; Burger, P.; Ruppli, U.; Berke, H. *Organometallics* **1994**, *13*, 4203. (c) Crabtree, R. H.; Lavin, M.; Bonneviot, L. *J. Am. Chem. Soc.* **1986**, *108*, 4032. (d) Castillo, A.; Barea, G.; Esteruelas, M. A.; Lahoz, F. J.; Lledós, A.; Maseras, F.; Modrego, J.; Onate, E.; Oro, L. A.; Ruiz, N.; Sola, E. *Inorg. Chem.* **1999**, *38*, 1814. (e) Taw, F. L.; Mellows, H.; White, P. S.; Hollander, F. J.; Bergman, R. D.; Brookhart, M.; Heinekey, D. M. *J. Am. Chem. Soc.* **2002**, *124*, 5100. (f) Cooper, A. C.; Eisenstein, O.; Caulton, K. G. *New J. Chem.* **1998**, *22*, 307. (g) Sabo-Etienne, S.; Rodriguez, V.; Donnadieu, B.; Chaudret, B.; Makarim, H. A.; Barthelat, J.; Ulrich, S.; Limbach, H.; Moise, C. *New J. Chem.* **2001**, *25*, 55. (h) Camanyes, S.; Maseras, F.; Moreno, M.; Lledós, A.; Lluch, J. M.; Bertrán, J. *J. Am. Chem. Soc.* **1996**, *118*, 4617.

(9) Herrmann, W. A.; Okuda, J. *Angew. Chem., Int. Ed. Engl.* **1986**, *25*, 1092.

(10) Herrmann, W. A.; Theiler, H. G.; Herdtweck, E.; Kiprof, P. *J. Organomet. Chem.* **1989**, *367*, 291.

(11) Costello, M. T.; Fanwick, P. E.; Green, M. A.; Walton, R. A. *Inorg. Chem.* **1992**, *31*, 2359.

(12) Loren, S. D.; Campion, B. K.; Heyn, R. H.; Tilley, T. D.; Bursten, B. E.; Luth, K. W. *J. Am. Chem. Soc.* **1989**, *111*, 4712.

(13) Fagan, P. J.; Ward, M. D.; Calabrese, J. C. *J. Am. Chem. Soc.* **1989**, *111*, 1698.

dryness. The residue was purified by column chromatography on alumina with toluene/diethyl ether (5/1) to give **6** (36.7 mg, 0.0652 mmol, 42%).

Cp'Ru(μ -H)₃ReH(triphos) (9). A solution of (triphos)ReH₅ (384.9 mg, 0.477 mmol) and (Cp'RuOMe)₂ (134.0 mg, 0.250 mmol) in toluene was stirred at room temperature for 12 h. The solution turned from purple to brown. The solvent was then removed under reduced pressure. The residue was extracted with toluene, and the extract was purified by column chromatography on alumina with toluene. The red fraction was collected and evaporated to dryness to afford complex **9** as a brown solid (455.3 mg, 0.433 mmol, 91%). ¹H NMR (400 MHz, C₆D₆, room temperature, δ /ppm): 7.72 (m, 12H, *Ph*), 6.87 (t, $J_{\text{HH}} = 7.4$ Hz, 12H, *Ph*), 6.79 (t, $J_{\text{HH}} = 7.4$ Hz, 6H, *Ph*), 2.22 (s, 15H, *Cp'*), 2.12 (br, 6H, *CH₂*), 1.13 (d, $J_{\text{PH}} = 2.4$ Hz, 3H, *Me*), -9.66 (q, $J_{\text{PH}} = 8.3$ Hz, 4H, μ -*H* and *Re-H*). ¹³C NMR (100 MHz, C₆D₆, room temperature, δ /ppm): 142.8 (dt, $J_{\text{PC}} = 46.3, 18.7$ Hz, *Ph*), 132.6 (d, $J_{\text{CH}} = 163.5$ Hz, *Ph*), 132.2 (d, $J_{\text{CH}} = 159.3$ Hz, *Ph*), 127.2 (d, $J_{\text{CH}} = 164.8$ Hz, *Ph*), 80.8 (s, C₅Me₅), 42.5 (s, CH₃C(CH₂)₃), 37.8 (q, $J_{\text{CH}} = 124.5$ Hz, CH₃C(CH₂)₃), 35.0 (t, $J_{\text{CH}} = 122.4$ Hz, CH₃C(CH₂)₃), 13.2 (q, $J_{\text{CH}} = 125.1$ Hz, C₅Me₅). ³¹P{¹H} NMR (168 MHz, THF-*d*₆, room temperature, δ /ppm): 16.0 (PPh₂). IR (ATR, cm⁻¹): 3054, 2955, 1939, 2899, 2859, 1964 ($\nu_{\text{Re-H}}$), 1822, 1434, 1183, 1117, 1092, 1026, 999, 906. Anal. Calcd for C₅₁H₅₈P₃RuRe: C, 58.27; H, 5.56. Found: C, 58.63; H, 5.56.

[(Cp'Ru)₂(Cp'Re)(μ -H)₅][BF₄] (10a). To a diethyl ether solution of **6** (142.5 mg, 0.253 mmol) was added tetrafluoroboric acid-dimethyl ether complex (15 μ L). The black solid that precipitated from the solution was collected on a glass frit and washed with ether to give complex **10a** (112.2 mg, 0.126 mmol, 99%). From the washings unreacted Cp'ReH₆ was recovered by evaporation of the solvent and subsequent chromatographic purification. The C₅EtMe₄ analogue [(C₅EtMe₄Ru)₂(Cp'Re)(μ -H)₅][BF₄] (**10a'**), was prepared in a similar manner by the use of **6a'** as the starting material. **10a**: ¹H NMR (400 MHz, acetone-*d*₆, room temperature, δ /ppm) 2.32 (s, 15H, *Cp'*Re), 1.97 (s, 30H, *Cp'*Ru), -9.52 (br s, 1H, RuH/Ru), -11.31 (brs, 4H, RuH/Ru); ¹³C NMR (100 MHz, acetone-*d*₆, room temperature, δ /ppm) 97.8 (s, C₅Me₅Re), 92.4 (s, C₅Me₅Ru), 12.4 (q, $J_{\text{CH}} = 127.9$ Hz, C₅Me₅Re), 12.3 (q, $J_{\text{CH}} = 127.2$ Hz, C₅Me₅Ru); IR (ATR, cm⁻¹) 2987, 2964, 2942, 2935, 2926, 2918, 2911, 1557, 1455, 1428, 1382, 1261, 1094, 1052, 1024, 801. Anal. Calcd for C₃₀H₅₀BF₄Ru₂Re: C, 40.67; H, 5.67. Found: C, 40.42; H, 5.71. **10a'**: ¹H NMR (400 MHz, acetone-*d*₆, room temperature, δ /ppm) 2.45 (q, $J_{\text{HH}} = 7.5$ Hz, 4H, CH₃CH₂-), 2.32 (s, 15H, *Cp'*Re), 1.98 (s, 12H, C₅EtMe₄Ru), 1.97 (s, 12H, C₅EtMe₄Ru), 1.11 (t, $J_{\text{HH}} = 7.5$ Hz, 6H, CH₃CH₂-), -9.60 (brs, 1H, RuH/Ru), -11.27 (brs, 4H, RuH/Ru); ¹³C NMR (100 MHz, acetone-*d*₆, room temperature, δ /ppm) 97.9 (s, C₅Me₅Re), 97.4 (s, C₅EtMe₄Ru), 92.7 (s, C₅EtMe₄Ru), 92.1 (s, C₅EtMe₄Ru), 20.7 (t, $J_{\text{CH}} = 128.2$ Hz, C₅EtMe₄Ru), 14.6 (q, $J_{\text{CH}} = 126.7$ Hz, C₅EtMe₄Ru), 12.4 (q, $J_{\text{CH}} = 127.9$ Hz, C₅Me₅Re), 12.3 (q, $J_{\text{CH}} = 127.4$ Hz, C₅EtMe₄Ru), 12.1 (q, $J_{\text{CH}} = 127.4$ Hz, C₅EtMe₄Ru); IR (ATR, cm⁻¹) 3053, 3031, 3013, 2999, 2983, 2907, 1578, 1477, 1425, 1376, 1256, 1148, 1067, 1021. Anal. Calcd for C₃₂H₅₄BF₄Ru₂Re: C, 42.06; H, 5.96. Found: C, 42.24; H, 6.38.

[(Cp'Ru)₂(Cp'Re)(μ -H)₅][BPh₄] (10b). To a methanol solution of **10a** (25.2 mg, 0.0284 mmol) was added sodium tetraphenylborate. Immediately, a black solid was formed, and the supernatant was then removed by decantation. The resulting solid was washed with methanol and dried under reduced pressure to afford **10b** (26.5 mg, 0.0237 mmol, 83%) as a purple solid. The C₅EtMe₄ analogue [(C₅EtMe₄Ru)₂(Cp'Re)(μ -H)₅][BPh₄] (**10b'**) was prepared in a similar manner by using **10a'** instead of **10a**. **10b**: ¹H NMR (400 MHz, acetone-*d*₆, room temperature, δ /ppm) 7.34 (m, 8H, *Ph*), 6.92 (t, $J_{\text{HH}} = 7.1$ Hz, 8H, *Ph*), 6.78 (t, $J_{\text{HH}} = 7.1$ Hz, 4H, *Ph*), 2.30 (s, 15H, *Cp'*Re), 1.95 (s, 30H, *Cp'*Ru), -9.54 (br s, 1H, RuH/Ru), -11.32 (br s, 4H, RuH/Ru); ¹³C NMR (100 MHz, acetone-*d*₆, room temperature, δ /ppm) 164.2 (*Ph*), 137.0 (d, $J_{\text{CH}} = 151.7$ Hz, *Ph*),

125.9 (d, $J_{\text{CH}} = 150.9$ Hz, *Ph*), 122.2 (d, $J_{\text{CH}} = 155.4$ Hz, *Ph*), 97.8 (s, C₅Me₅Re), 92.4 (s, C₅Me₅Ru), 12.4 (q, $J_{\text{CH}} = 127.8$ Hz, C₅Me₅Re), 12.3 (q, $J_{\text{CH}} = 127.4$ Hz, C₅Me₅Ru); IR (ATR, cm⁻¹) 3053, 3032, 3014, 3000, 2983, 2907, 1701, 1578, 1478, 1426, 1376, 1256, 1148, 1067, 1012, 732, 705. Anal. Calcd for C₅₄H₇₀BRu₂Re: C, 58.00; H, 6.31. Found: C, 57.65; H, 7.00. **10b'**: ¹H NMR (400 MHz, acetone-*d*₆, room temperature, δ /ppm) 7.34 (m, 8H, *Ph*), 6.92 (t, $J_{\text{HH}} = 7.4$ Hz, 8H, *Ph*), 6.78 (t, $J_{\text{HH}} = 7.4$ Hz, 4H, *Ph*), 2.44 (q, $J_{\text{HH}} = 7.7$ Hz, 4H, *Et*), 2.30 (s, 15H, *Cp'*Re), 1.97 (s, 12H, C₅EtMe₄Ru), 1.96 (s, 12H, C₅EtMe₄Ru), 1.10 (q, $J_{\text{HH}} = 7.7$ Hz, 6H, *Et*), -9.61 (br s, 1H, RuH/Ru), -11.27 (br s, 4H, RuH/Ru); ¹³C NMR (100 MHz, acetone-*d*₆, room temperature, δ /ppm) 164.9 (q, $J_{\text{BC}} = 49$ Hz, *Ph*), 137.0 (d, $J_{\text{CH}} = 152.4$ Hz, *Ph*), 125.9 (d, $J_{\text{CH}} = 151.1$ Hz, *Ph*), 122.2 (d, $J_{\text{CH}} = 155.6$ Hz, *Ph*), 97.8 (s, C₅Me₅Re), 97.4 (s, C₅EtMe₄Ru), 92.7 (s, C₅EtMe₄Ru), 92.1 (s, C₅EtMe₄Ru), 20.7 (t, $J_{\text{CH}} = 128.3$ Hz, C₅EtMe₄Ru), 14.6 (q, $J_{\text{CH}} = 126.5$ Hz, C₅EtMe₄Ru), 12.4 (q, $J_{\text{CH}} = 128.0$ Hz, C₅Me₅Re), 12.3 (q, $J_{\text{CH}} = 127.4$ Hz, C₅EtMe₄Ru), 12.1 (q, $J_{\text{CH}} = 129.4$ Hz, C₅EtMe₄Ru); IR (ATR, cm⁻¹) 3054, 3033, 2982, 2913, 1580, 1471, 1455, 1423, 1377, 1263, 1083, 1024, 911, 845, 731, 703. Anal. Calcd for C₅₆H₇₄BRu₂Re: C, 58.67; H, 6.89. Found: C, 58.70; H, 6.98.

(Cp'Ru)₂(Cp'Re)(μ -H)₄ (7). Complex **10a** (112.2 mg, 0.126 mmol) and sodium methoxide (80.7 mg, 1.49 mmol) were dissolved in methanol, and the solution was stirred. After being stirred for 15 min, the solvent was removed under reduced pressure and the residue was extracted with toluene. The extract was filtered through a Celite pad. Evaporation of the solvent from the filtrate yielded **7** (90.6 mg, 0.114 mmol, 90%). The C₅EtMe₄ analogue [(C₅EtMe₄Ru)₂(Cp'Re)(μ -H)₄ (**7**)] was similarly prepared by using **10a'** instead of **10a**. **7**: ¹H NMR (400 MHz, C₆D₆, room temperature, δ /ppm) 2.14 (s, 15H, *Cp'*Re), 1.91 (s, 30H, *Cp'*Ru), -13.71 (s, 4H, μ -*H*); ¹³C NMR (100 MHz, C₆D₆, room temperature, δ /ppm) 91.5 (s, C₅Me₅Re), 79.9 (s, C₅Me₅Ru), 13.6 (q, $J_{\text{CH}} = 125.4$ Hz, C₅Me₅Ru), 13.1 (q, $J_{\text{CH}} = 126.4$ Hz, C₅Me₅Re); IR (ATR, cm⁻¹) 2961, 2849, 1497, 1373, 1263, 1072, 1026, 909, 884, 805. Anal. Calcd for C₃₀H₄₉Ru₂Re: C, 45.15; H, 6.19. Found: C, 44.96; H, 6.32. **7'**: ¹H NMR (400 MHz, C₆D₆, room temperature, δ /ppm) 2.51 (q, $J_{\text{HH}} = 7.4$ Hz, 4H, CH₃CH₂-), 2.15 (s, 15H, *Cp'*Re), 1.94 (s, 12H, C₅Me₄EtRu), 1.92 (s, 12H, C₅Me₄EtRu), 1.09 (t, $J_{\text{HH}} = 7.4$ Hz, 6H, CH₃CH₂-), -13.64 (s, 4H, μ -*H*); ¹³C NMR (100 MHz, C₆D₆, room temperature, δ /ppm) 91.6 (s, C₅Me₅Re), 85.5 (s, C₅Me₄EtRu), 80.4 (s, C₅Me₄EtRu), 79.3 (s, C₅Me₄EtRu), 21.9 (t, $J_{\text{CH}} = 128.9$ Hz, CH₃CH₂-), 14.9 (q, $J_{\text{CH}} = 125.9$ Hz, CH₃CH₂-), 13.5 (q, $J_{\text{CH}} = 125.4$ Hz, C₅Me₄EtRu), 13.4 (q, $J_{\text{CH}} = 125.4$ Hz, C₅Me₄EtRu), 13.1 (q, $J_{\text{CH}} = 126.1$ Hz, C₅Me₅Re); IR (ATR, cm⁻¹) 2963, 2904, 1471, 1372, 1261, 1088, 1025, 909, 801. Anal. Calcd for C₃₂H₅₃Ru₂Re: C, 46.52; H, 6.47. Found: C, 46.42; H, 6.77.

(Cp'Ru)(Cp'Re)₂(H)₅ (8). A solution of (Cp'ReH₃)₂ (23.0 mg, 0.0354 mmol) and (Cp'RuOMe)₂ (10.9 mg, 0.0204 mmol) in toluene (3 mL) was stirred at room temperature. After the mixture was stirred for 5 h, the solvent was removed under reduced pressure. The residue was extracted with tetrahydrofuran, and the extract was purified by column chromatography on alumina with tetrahydrofuran. The purple fraction was collected and evaporated to dryness to afford complex **8** as a brown solid (24.8 mg, 0.0281 mmol, 79%). The C₅EtMe₄ analogue (C₅EtMe₄Ru)(Cp'Re)₂(H)₅ (**8'**) was prepared in a similar manner in 70% yield by using (C₅EtMe₄RuOMe)₂. **8**: ¹H NMR (400 MHz, C₆D₆, room temperature, δ /ppm) 2.29 (s, 30H, *Cp'*Re), 1.73 (s, 15H, *Cp'*Ru), -12.67 (s, 5H, *hydride*); ¹³C NMR (100 MHz, C₆D₆, room temperature, δ /ppm) 91.0 (s, C₅Me₅Re), 81.0 (s, C₅Me₅Ru), 13.5 (q, $J_{\text{CH}} = 125.9$ Hz, C₅Me₅Ru), 13.1 (q, $J_{\text{CH}} = 125.6$ Hz, C₅Me₅Re); IR (ATR, cm⁻¹) 2961, 2904, 2849, 1447, 1373, 1263, 1072, 1026, 909, 884. Anal. Calcd for C₃₀H₅₀RuRe₂: C, 40.75; H, 5.70. Found: C, 40.28; H, 5.60. **8'**: ¹H NMR (400 MHz, C₆D₆, room temperature, δ /ppm) 2.35 (q, $J_{\text{HH}} = 7.9$ Hz, 2H, CH₃CH₂-), 2.29 (s, 30H, *Cp'*Re), 1.76 (s, 6H, C₅Me₄EtRu), 1.73 (s, 6H, C₅Me₄EtRu), 0.99 (t, $J_{\text{HH}} = 7.5$

Table 1. Crystallographic Data for **6**, **7'**, **9**, and **10b'**

	6	7'	10b'	9
formula	C ₂₀ H ₃₀ RuRe	C ₃₂ H ₅₃ Ru ₂ Re	C ₅₉ H ₈₀ BOReRu ₂	C ₅₁ H ₅₈ P ₃ ReRu
cryst descriptn	prism	block	prism	prism
cryst color	red	red	red	red
cryst size	0.4 × 0.4 × 0.4	0.3 × 0.3 × 0.3	0.4 × 0.2 × 0.1	0.3 × 0.2 × 0.2
crystallizing soln	<i>n</i> -pentane	<i>n</i> -pentane	acetone	<i>n</i> -heptane
cryst syst	monoclinic	monoclinic	triclinic	orthorhombic
space group	<i>P</i> 2 ₁ / <i>n</i> (No. 14)	<i>P</i> 2 ₁ / <i>n</i> (No. 14)	<i>P</i> 1̄ (No. 2)	<i>Pbca</i> (No. 61)
<i>a</i> , Å	8.0931(2)	10.880(5)	10.528(4)	21.9663(5)
<i>b</i> , Å	18.8274(5)	23.167(9)	14.646(6)	34.3599(17)
<i>c</i> , Å	14.1609(4)	12.783(6)	17.551(8)	12.1515(6)
α, deg			84.17(3)	
β, deg	100.9650(9)	100.03(4)	88.75(4)	
γ, deg			89.36(4)	
<i>V</i> , Å ³	2118.33(10)	3173(2)	2692(2)	9171.5(7)
<i>Z</i>	4	4	2	8
<i>D</i> _{calcd} , g cm ⁻³	1.765	1.729	1.486	1.523
temp, °C	-50	-100	-100	-50
μ(Mo Kα), mm ⁻¹	6.419	4.763	2.835	3.105
diffractometer	R-AXIS RAPID	R-AXIS RAPID	R-AXIS RAPID	R-AXIS CS
radiation		Mo Kα (λ = 0.710 69 Å)		
monochromator		graphite		
2θ _{max} , deg	60	55	55	55
no. of rflns collected	25 697	28 413	27 168	76 882
no. of indep rflns	6108	6351	11 470	7151
no. of rflns obsd (> 2σ)	5479	6351	10535	5756
abs cor type	numerical	empirical	empirical	numerical
abs transmissn, min/max	0.2163/0.3154	0.7319/1.0000	0.4409/1.2830	0.7543/0.8498
R1 (<i>I</i> > 2σ(<i>I</i>))	0.0483	0.0294	0.0865	0.0296
wR2 (<i>I</i> > 2σ(<i>I</i>))	0.1230	0.0621	0.2256	0.0584
R1 (all data)	0.0532	0.0294	0.0921	0.0455
wR2 (all data)	0.1263	0.0621	0.2316	0.0609
no. of restraints	2	0	0	6
no. of params	230	286	595	527
GOF	1.064	1.133	1.066	1.006

Hz, 3H, CH₃CH₂-), -12.66 (s, 5H, *hydride*); ¹³C NMR (100 MHz, C₆D₆, room temperature, δ/ppm) 91.0 (s, C₅Me₅Re), 86.5 (s, C₅Me₄EtRu), 81.4 (s, C₅Me₄EtRu), 80.6 (s, C₅Me₄EtRu), 22.0 (t, *J*_{CH} = 125.2 Hz, CH₃CH₂-), 14.7 (q, *J*_{CH} = 125.8 Hz, CH₃CH₂-), 13.4 (q, *J*_{CH} = 124.6 Hz, C₅Me₄EtRu), 13.3 (q, *J*_{CH} = 125.9 Hz, C₅Me₄EtRu), 13.1 (q, *J*_{CH} = 125.6 Hz, C₅Me₅Re); IR (ATR, cm⁻¹) 2962, 2904, 1471, 1372, 1261, 1087, 1025, 909, 801. Anal. Calcd for C₃₁H₅₂RuRe₂: C, 41.45; H, 5.83. Found: C, 41.59; H, 6.02.

Protonation of 6. An NMR sample tube was charged with **6** (6.4 mg, 0.011 mmol) and tetrahydrofuran-*d*₈ (0.5 mL) and cooled to -196 °C. To the sample was added tetrafluoroboric acid-dimethyl ether complex (15 μL, 0.12 mmol). The reaction was monitored by means of ¹H NMR spectroscopy at -80 °C. The spectrum reveals the formation of **10a**, Cp'ReH₆, and [(Cp'Ru)₂(Cp'Re)₂H₁₁]⁺ (**A**) in the ratio 1:1:0.22. With an increase in temperature, the signal of [(Cp'Ru)₂(Cp'Re)₂H₁₁]⁺ disappeared and those of **10a** and Cp'ReH₆ increased. Notably, the ratio between **10a** and Cp'ReH₆ was ca. 1:1, irrespective of the elapsed time. **A**: ¹H NMR (400 MHz, THF-*d*₈, -80 °C, δ/ppm) 2.48 (s, 30H, Cp'), 1.82 (s, 30H, Cp'), -8.61 (br s, 11H, μ-*H*); ¹³C{¹H} NMR (100 MHz, THF-*d*₈, -80 °C, δ/ppm) 104.2 (C₅Me₅), 87.3 (C₅Me₅), 11.9 (C₅Me₅), 11.7 (C₅Me₅).

Reaction of 6 with HBF₄ in Toluene. Upon addition of 1 equiv of HBF₄(OMe₂) to a solution of **6** in toluene (8.5 × 10⁻³ M) at -78 °C followed by warming to room temperature, the solution turned from brown to purple and a solid was precipitated. The solution was removed under reduced pressure. The residue was dissolved in chloroform-*d*, and the ¹H NMR spectrum was recorded. The spectrum showed the formation of **10a**, Cp'ReH₆, and [Cp'Ru(*η*⁶-C₆H₅CH₃)](BF₄) in the ratio of 1.0:0.74:0.05.

H/D Exchange of Hydride Ligands in 6, 7, 8, and 10a with D₂. Roto Tite NMR sample tubes were charged with 0.4 mL of THF-*d*₈ and complexes **7**, **8**, and **10a**, separately. After the headspace of the NMR tube was evacuated at -196 °C, D₂ was admitted. The samples were then warmed to room

temperature and the reactions were monitored by ¹H NMR spectroscopy. The time-exchange rates are given in the Supporting Information. The H/D exchange reaction proceeded for **7**, **8**, and **10a** even at room temperature. In contrast, no reaction proceeded when **6** was heated to 80 °C in C₆D₆.

H/D Exchange with C₆D₆. Roto Tite NMR sample tubes were charged with 0.4 mL of C₆D₆ and complexes **7**–**9**, separately. The H/D exchange reaction was monitored at 80 °C by means of ¹H NMR spectroscopy. The results are given in the Supporting Information.

X-ray Diffraction Studies. Single crystals of **6**, **7'**, and **10b'** for an X-ray analysis were mounted on a Rigaku R-AXIS RAPID imaging plate diffractometer equipped with a graphite-monochromated Mo Kα source (λ = 0.710 69 Å). Data were collected on 55 oscillation images with oscillation range of 4° for **6** and on 44 oscillation images with an oscillation range of 5° for **7'** and **10b'**. A single crystal of **9** for an X-ray analysis was mounted on a Rigaku R-AXIS CS imaging plate diffractometer equipped with a graphite-monochromated Mo Kα source (λ = 0.710 69 Å). Data were collected on 60 oscillation images with an oscillation range of 4° and overlap range of 1°. In all samples, cell refinement and data reduction were performed using the PROCESS-AUTO program.¹⁴ Intensity data were corrected for Lorentz-polarization effects and for numerical or empirical absorption.

The structure of **6** was solved by the direct method using the SHELXS-97 program package.¹⁵ The structures of **7'** and **10b'** were solved by the Patterson method using the SHELXS-97 program package. The structure of **9** was also solved by the Patterson method (DIRDIF92-PATY) using the teXsan program package.¹⁶ Non-hydrogen atoms were found by Fourier syntheses. The refinement was carried out by least-squares methods based on *F*² with all measured reflections (SHELXL-97).¹⁷ For **7'**, disorder at the C₅EtMe₄ ligand bonded

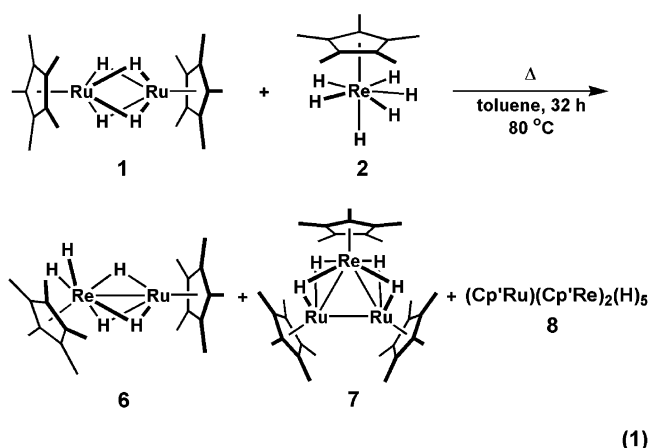
(14) PROCESS-AUTO: Automatic Data Acquisition and Processing for Imaging Plate Diffractometer; Rigaku Corp., Tokyo, Japan, 1998.

to the Ru₂ atom was refined in the ratio of 52:48. The hydrogen atoms, except those bonded to metals, were included in calculated positions and refined by using a riding mode. The metal-bound hydrogen atoms of **6** and **9** were located in difference Fourier maps and refined with restraint. The metal-bound hydrogen atoms of **7'** were located in a difference Fourier map and refined isotropically. Refinement converged with allowance for thermal anisotropy of all non-hydrogen atoms in both complexes. Details of crystal data and data collection and refinement parameters are summarized in Table 1.

Results and Discussion

Synthesis of Heterobimetallic Polyhydride Complex. Previously, we reported that the diruthenium tetrahydride complex Cp'Ru(μ-H)₄RuCp' (**1**)^{1a} was a suitable precursor for the synthesis of a heterobimetallic polyhydride complex containing ruthenium and iridium.^{5a} The heterobimetallic polyhydride Cp'Ru(μ-H)₃IrCp' was obtained in reasonable yield in the reaction of the diruthenium tetrahydride **1** with the mononuclear iridium polyhydride Cp'IrH₄. This method, namely, coupling of two metal fragments by way of intermolecular dehydrogenation, is a useful and practical method for the synthesis of the heterometallic polyhydride complex. We applied this method to the synthesis of new heteronuclear cluster complexes having a metal–metal bond between ruthenium and rhenium. We adopted a mononuclear polyhydride of rhenium, Cp'ReH₆ (**2**), as the source of the rhenium fragment in the Ru–Re heterobimetallic polyhydride cluster.

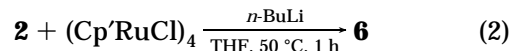
The reaction of **2** with 1/2 mol of **1** in toluene at 80 °C resulted in the formation of a mixture of Cp'Ru(μ-H)₃ReH₂Cp' (**6**), (Cp'Ru)₂(Cp'Re)(μ-H)₄ (**7**), and (Cp'Ru)(Cp'Re)₂(H)₅ (**8**) (eq 1). Only the binuclear complex **6** was



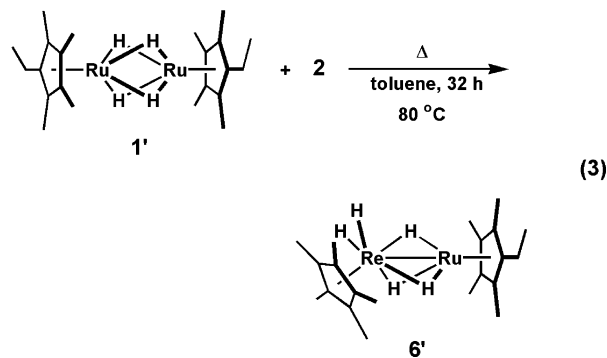
isolated in 53% yield by column chromatography on alumina. The trinuclear complexes **7** and **8** were, however, not separable, unfortunately. Therefore, they were prepared by an alternative method (vide infra).

Complex **6** was alternatively synthesized by treatment of a mixture of (Cp'RuCl)₄ and 4 mol amounts of

Cp'ReH₆ with *n*-BuLi in tetrahydrofuran at 50 °C (eq 2).



Complex **6** has a C₅Me₅ ligand on both the ruthenium and rhenium centers. The Ru–Re heterobimetallic cluster (C₅Me₄Et)Ru(μ-H)₃ReH₂Cp' (**6'**), which has a different type of cyclopentadienyl ligand on each of the metal centers, was synthesized in a similar manner by the use of (C₅Me₄Et)Ru(μ-H)₄Ru(C₅Me₄Et) instead of Cp'Ru(μ-H)₄RuCp' for the sake of assignment of the C₅Me₅ signals in both the ¹H and ¹³C NMR spectra of complex **6** (vide infra) (eq 3).



The ¹H NMR spectrum shows that **6** is fluxional and the shape of the signals is significantly dependent on the temperature. In the ¹H NMR spectrum of **6** measured in C₆D₆ at room temperature, two Cp' signals were observed at δ 1.84 (15 H) and 2.14 (15 H). The former is unambiguously assigned to the Cp' group on the ruthenium atom, in comparison with the data for the analogous bimetallic polyhydride clusters Cp'Ru(μ-H)₄RuCp' (δ 1.86),^{1a} CpRu(μ-H)₃IrCp' (δ 1.90),^{5a} Cp'Ru(μ-H)₃W(H)₃Cp' (δ 1.88), and Cp'Ru(μ-H)₃Mo(H)₃Cp' (δ 1.94).^{5b} The latter is, therefore, assigned to the Cp' group bound to the rhenium atom. The assignment of these signals was proved to be reasonable by comparison with the data for the labeled compound (C₅Me₄Et)Ru(μ-H)₃ReH₂Cp' (**6'**). In the ¹H NMR spectrum of **6'**, three singlet peaks and a set of triplet and quartet peaks appeared at δ 1.85 (6H), 1.86 (6H), 2.14 (15 H), 1.05 (t, *J* = 7.6 Hz, 3H), and 2.38 (q, *J* = 7.6 Hz, 2H), respectively. The two singlet signals with intensity of 6H and a set of the triplet and quartet signals are due to the C₅Me₄Et group coordinated to the ruthenium atom, and the singlet observed at δ 2.14 is ascribed to the Cp' group bound to the rhenium atom. Thus, the assignment of ¹H signals for **6** is consistent with that for **6'**.

As mentioned above, the fluxional behavior of complex **6** was revealed in the ¹H NMR spectra measured at various temperatures. The hydride regions of the spectra, δ –10.5 to –11.5 ppm, recorded in the temperature range from +20 to –110 °C are shown in Figure 1.

At 20 °C, the five hydride ligands were observed to be equivalent at δ –10.90 ppm. With a decrease in the temperature, a significant broadening of the signal was observed. Then the signal decoalesced and split into two peaks with an intensity ratio of 2:3. The broad singlet peaks observed at δ –10.94 (2H) and –10.99 (3H) were assigned to the resonances for the terminal hydrides

(15) Sheldrick, G. M. SHELXS-97: Program for the Solution of Crystal Structures; University of Göttingen, Göttingen, Germany, 1997.

(16) teXsan: Single-Crystal Structure Analysis Software; Molecular Structure Corp., The Woodlands, TX, and Rigaku Corp., Tokyo, Japan, 1992.

(17) Sheldrick, G. M. SHELXL-97. Program for the Refinement of Crystal Structures; University of Göttingen, Göttingen, Germany, 1997.

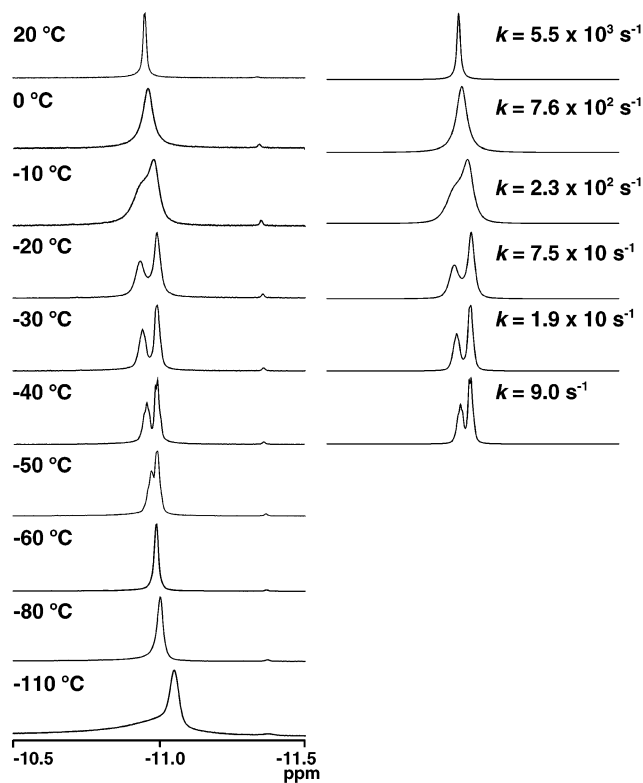


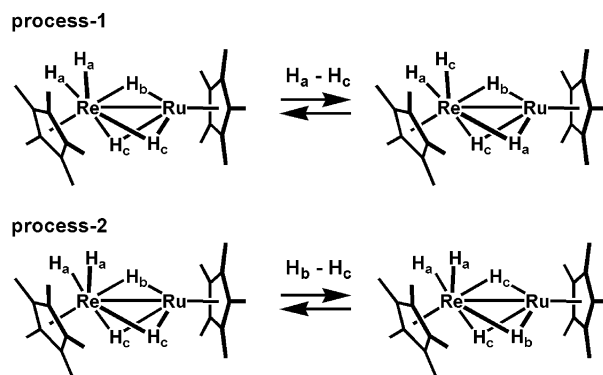
Figure 1. Experimental (left) and simulated (right) variable-temperature ^1H NMR spectra of **6** showing the region of the hydride protons.

bound to the rhenium atom and the bridging hydrides, respectively. Whereas the signal for the terminal hydrides gradually shifts upfield with a fall in the temperature, the chemical shift for the bridging hydrides remained almost unchanged, even though significant broadening of the signal was observed. The chemical shifts of these two peaks, namely, signals for the terminal hydrides and the bridging hydrides, reversed at about below $-60\text{ }^\circ\text{C}$, and a slightly broad signal for the terminal hydrides was observed upfield from that for the bridging hydrides. The change in the chemical shift of the terminal hydride depended on temperature, with a linear correlation in the range from -20 to $-110\text{ }^\circ\text{C}$ (Figure S1 in the Supporting Information). The significant broadening of the signal for the bridging hydrides is most likely due to a slowdown in the rate of site exchange between *cis*-H (H_c) and *trans*-H (H_b) with respect to the C_5Me_5 group on the rhenium atom.

The dynamic behavior of **6** includes two processes in all, namely, site exchange of the hydrides between the terminal and bridging positions (process 1) and site exchange among the bridging hydrides (process 2) (Scheme 1). In both process 1 and process 2, one of the possible intermediates or transient species is an $\eta^2\text{-H}_2$ complex formed as a result of a bonding interaction between the two hydride ligands which exchange coordination sites.^{8a}

We could not estimate the activation parameters for process 2, because the slow exchange limit spectrum was not obtained even at $-110\text{ }^\circ\text{C}$. The activation parameters for process 1 were, however, obtained as a result of simulation of the line shape of the spectra in the temperature range from $+20$ to $-40\text{ }^\circ\text{C}$ in consideration of the temperature dependence of the hydride signals,

Scheme 1



as mentioned above. As a result, the enthalpy, entropy, and free energy of activation were estimated to be $\Delta H^\ddagger = 15.5\text{ kcal mol}^{-1}$, $\Delta S^\ddagger = 11.5\text{ cal mol}^{-1}\text{ K}^{-1}$, and $\Delta G^\ddagger_{298\text{ K}} = 12.1\text{ kcal mol}^{-1}$, respectively.

A characteristic reaction of the polyhydride complex is an intermolecular H/D exchange reaction between the hydride ligands and deuterated substrates such as D_2 and C_6D_6 . The mechanistic studies of the intermolecular H/D exchange reaction proved that the reaction proceeded via an oxidative addition of the deuterated substrate.¹⁸

Both the site exchange of the hydride ligands and the intermolecular H/D exchange reactions of the polyhydride complexes proceed by way of a common reaction intermediate, namely, the $\eta^2\text{-H}_2$ species. The activity of the H/D exchange reaction, therefore, seems closely related to the capability for intramolecular site exchange of the hydride ligands.

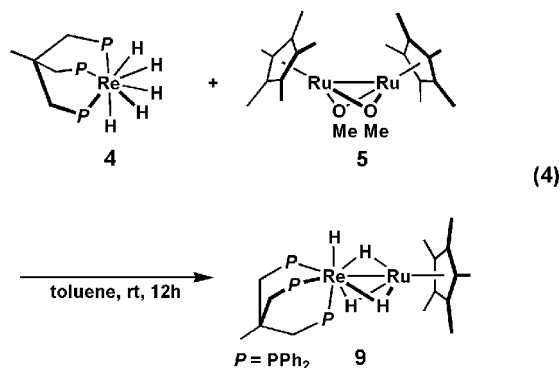
As anticipated from the relatively large free energy of activation for the site exchange reaction of the hydride ligands, complex **6** was resistant to the H/D exchange reaction between both D_2 and C_6D_6 under mild conditions. A solution of **6** in C_6D_6 was heated to $80\text{ }^\circ\text{C}$ under 1 atm of D_2 , and the change in the integral intensity of the hydride signal was monitored by ^1H NMR spectroscopy. The spectrum, however, remained unchanged after heating for 25 h, and the H/D exchange reaction did not proceed with either D_2 or C_6D_6 . Such a positive correlation between the kinetic parameters for the site exchange reaction of the hydride ligands and the feasibility of the intermolecular H/D exchange reaction was also indicated for the heterobimetallic complex $\text{Cp}^*\text{Ru}(\mu\text{-H})_3\text{ReH}(\text{triphos})$ (**9**). Complex **9**, which has a relatively small free energy of activation for the site exchange, readily undergoes an H/D exchange reaction with both D_2 and C_6D_6 at ambient temperature (vide infra).

Synthesis of a Heterobimetallic Polyhydride Complex Having a Tridentate Phosphine Ligand on the Rhenium Atom. The cyclopentadienyl (C_5R_5) ligand can be a full $\eta^5\text{-C}_5\text{R}_5$ five-electron donor or, in a "slipped" structure, an $\eta^3\text{-C}_5\text{R}_5$ three-electron donor. However, it is not so mobile as to change the coordination mode freely. In contrast, a tripod-type tridentate

(18) (a) Zeiher, E. H. K.; DeWit, D. G.; Caulton, K. G. *J. Am. Chem. Soc.* **1984**, *106*, 7006. (b) Jones, W. D.; Feher, F. J. *J. Am. Chem. Soc.* **1984**, *106*, 1650. (c) Abugideiri, F.; Fettingler, J. C.; Pleune, B.; Poli, R. *Organometallics* **1997**, *16*, 1179. (d) Jones, W. D.; Rosini, G. P.; Maguir, J. A. *Organometallics* **1999**, *18*, 1754. (e) Churchill, D. G.; Janak, K. E.; Wittenberg, J. S.; Parkin, G. *J. Am. Chem. Soc.* **2003**, *123*, 1403.

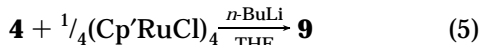
ligand such as $\text{CH}_3\text{C}(\text{CH}_2\text{PPh}_2)_3$ (triphos) possibly has enough flexibility to generate a vacant coordination site, due to a change in its denticity from tridentate to bidentate. Substitution of the Cp' ligand with triphos probably induces considerable change in the steric and electronic environment around the rhenium center and, as a result, directly affects the fluxional behavior of the hydride ligands and the generation of vacant coordination sites.

So far, there have been no precedents for the heterobimetallic polyhydride cluster, which has both the Cp' and the triphos groups in a molecule as the auxiliary ligands. We successfully synthesized the new heterobimetallic cluster $\text{Cp}'\text{Ru}(\mu\text{-H})_3\text{ReH}(\text{triphos})$ (**9**) and investigated the dynamic behavior of both the hydride and triphos ligands. The reaction of $(\text{triphos})\text{ReH}_5$ (**4**) with $(\text{Cp}'\text{RuOMe})_2$ (**5**) in toluene at room temperature resulted in the exclusive formation of the heterometallic binuclear complex $\text{Cp}'\text{Ru}(\mu\text{-H})_3\text{ReH}(\text{triphos})$ (**9**), which was isolated in 91% yield by column chromatography on alumina (eq 4). Formation of methanol in this



reaction was confirmed upon monitoring the reaction by ^1H NMR spectroscopy.

Complex **9** was alternatively synthesized by the use of $(\text{Cp}'\text{RuCl})_4$ as a precursor. The reaction of $(\text{Cp}'\text{RuCl})_4$ with $(\text{triphos})\text{ReH}_5$ in tetrahydrofuran at room temperature in the presence of a base such as *n*-BuLi or LiBEt_3H afforded **9** in high yield (eq 5).



Complex **9** is a highly air- and moisture-sensitive red solid and is soluble in a wide range of solvents from nonpolar to polar, such as benzene, toluene, pentane, ether, and acetonitrile.

Compound **9** was identified on the basis of its ^1H NMR spectral data. The spectrum exhibits fluxionality that is significantly dependent on the temperature. At room temperature, the methyl signal of the Cp' group was observed at δ 2.22 (15 H) and the signal of the hydrides was observed to be equivalent at δ -9.66 (4 H) as a quartet with coupling with the three phosphorus nuclei ($J_{\text{PH}} = 8.3$ Hz), due to the rapid exchange of the coordination sites among the hydride ligands (Figure 2). With a decrease in the temperature, the signal was broadened and split into two broad signals at -90 °C. Then, the signals gradually narrowed as the temperature fell. At -110 °C, two signals with intensities of 1H and 3H were observed at δ -7.88 and -10.65, respectively. The former is ascribed to the terminal hydride bound to the rhenium center, and the latter is assigned

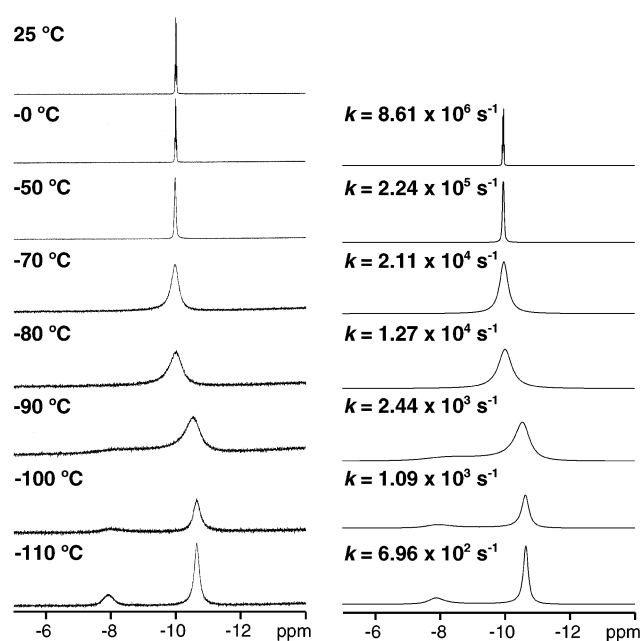


Figure 2. Experimental (left) and simulated (right) variable-temperature ^1H NMR spectra of **9** showing the region of the hydride protons.

to the bridging hydrides. At this temperature, the resonance for the three bridging hydrides is not sufficiently resolved. This shows that the three bridging hydrides still exchange coordination sites with one another: namely, *cis* and *trans* sites with respect to the terminal hydride.

The signals on the left-hand side of Figure 2 are the experimental set, and the right-hand side shows the signals simulated on the basis of the mechanism in Scheme 2.

The activation parameters were estimated by a line-shape analysis using the gNMR program. The derived ΔH^\ddagger and ΔS^\ddagger values for this dynamic process were 7.4 ± 0.4 kcal mol $^{-1}$ and -0.22 ± 0.22 cal mol $^{-1}$ K $^{-1}$, respectively. The free energy of activation at 298 K ($\Delta G^\ddagger_{298\text{ K}}$) is 7.5 kcal mol $^{-1}$, and this value is significantly smaller than those of **6** ($\Delta G^\ddagger_{298\text{ K}} = 12.1$ kcal mol $^{-1}$) and $(\text{CO})(\text{PPh}_3)_2\text{Re}(\mu\text{-H})_3\text{IrH}(\text{PPh}_3)_2$ ($\Delta G^\ddagger_{298\text{ K}} = 13$ kcal mol $^{-1}$).^{3a} Thus, the hydride ligands in **9** are very mobile in comparison to those in **6** and such mobility of the hydrides probably reflects the feasibility of forming an intermediary $\eta^2\text{-H}_2$ species.

The $^{31}\text{P}\{^1\text{H}\}$ NMR spectrum also exhibits fluxionality, and the temperature dependence of the spectrum is shown in Figure 3. Only a sharp singlet signal was observed at δ 16.0 at room temperature. This is likely due to equalization of circumstances of the three phosphorus nuclei concomitant with the rapid site exchange of the hydride ligands. As the temperature decreased, the signal gradually broadened. Below -110 °C, the signal decoalesced and split into two extremely broad peaks. Although the spectrum had not yet reached the slow exchange limit spectrum at -125 °C, two separated broad peaks with the intensity ratio 1:2 were observed at δ 20.6 ($w_{1/2} = 940$ Hz) and 12.5 ($w_{1/2} = 830$ Hz). They could be assigned to the phosphines *trans* and *cis*, respectively, with respect to the terminal hydride bound to the rhenium center. The activation parameters for the fluxional behavior of the triphos ligand were obtained as a result of simulation of the line shape of the spectra

Scheme 2

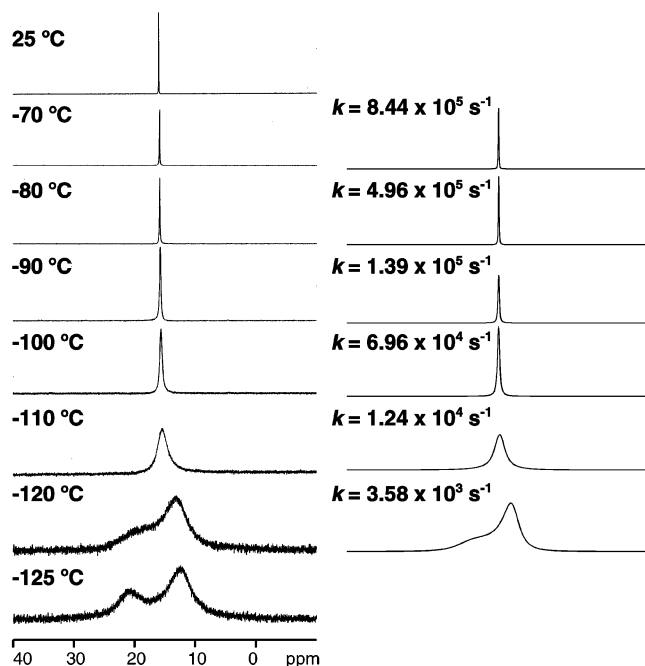
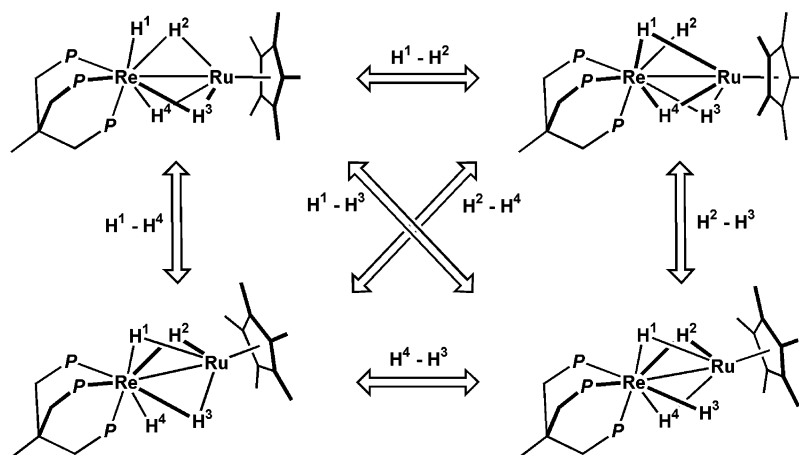


Figure 3. Experimental (left) and simulated (right) variable-temperature $^{31}\text{P}\{^1\text{H}\}$ NMR spectra of **9** showing the region of the triphos ligand.

in the temperature range from +25 to -120 °C. The enthalpy and entropy of activation were estimated to be $\Delta H^\ddagger = 6.7 \pm 0.3$ kcal mol⁻¹ and $\Delta S^\ddagger = 2.2 \pm 1.9$ cal mol⁻¹ K⁻¹, respectively. These activation parameters are very similar to those obtained for the site exchange of the hydrides within experimental error. This strongly indicates that the dynamic behavior of the triphos ligand and is most likely linked to the hydride scrambling process, as depicted in Scheme 2.

The H/D exchange reaction proceeds between complex **9** and C₆D₆. Not only hydride ligands but also hydrogen atoms in the phenyl groups of the triphos ligand were exchanged for deuterium atoms upon heating **9** to 80 °C in C₆D₆. The reaction was monitored by means of ¹H NMR spectroscopy, and the time–conversion rate curves for the hydride, *o*-H, *m*-H, and *p*-H are shown in Figure 4. The conversion rates are normalized. With the progress of the reaction, signals of the isotomers **9**-*d_n* (*n* = 0–3) were observed in the hydride region and the sum of the integral intensity of these signals gradually decreased.

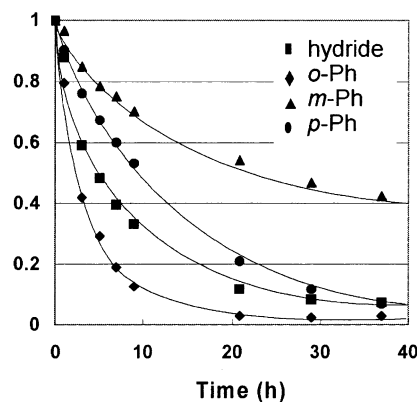


Figure 4. Time–conversion curve of the H/D reaction of **9** with C₆D₆.

The H/D exchange of the hydride ligands most certainly proceeded via coordination of C₆D₆ in an η^2 fashion to the vacant site, oxidative addition of C₆D₆, and subsequent reductive elimination of C₆D₅H. The vacant site would be generated as a result of a change in the coordination site of the hydride from bridge to terminal sites.

The exchange rate of the hydrogen atoms in the phenyl group is in the order of *o*-H > *p*-H > *m*-H. It is reasonable to assume that exchange of *o*-H is an intramolecular process and that of *m*- and *p*-H is an intermolecular process. We examined the concentration dependence of the exchange rate for *o*-, *m*-, and *p*-H in the range from 0.035 to 0.0075 M. The rates for *m*- and *p*-H noticeably decrease with a decrease in the concentration, whereas that for *o*-H was independent. This fact strongly indicates that H/D exchange for *m*- and *p*-H is an intermolecular process.¹⁹ The relatively slow exchange for *m*-H in comparison to that for *p*-H probably reflects the steric hindrance in the intermolecular oxidative addition. *o*-H of the phosphinophenyl group is exchanged via ortho metalation for the deuteride that resulted from intermolecular exchange between the hydride and C₆D₆. Such an intramolecular exchange between the hydride and *o*-H of the phosphinophenyl group has been reported by Caulton et al.^{3f}

Molecular Structures of **6 and **9**.** The molecular structures of **6** and **9** were determined by X-ray diffraction studies. Single crystals of **6** and **9** were obtained

(19) Jones, W. D.; Fan, M. *Organometallics* **1986**, *5*, 1057.

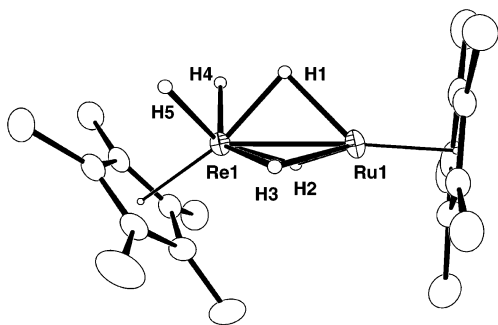


Figure 5. ORTEP diagram of the solid-state molecular structure of **6** with 30% probability ellipsoids. Selected bond length (Å): Ru(1)–Re(1) = 2.4798(5).

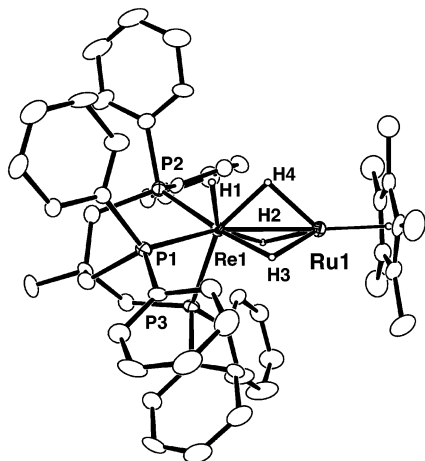


Figure 6. ORTEP diagram of the solid-state molecular structure of **9** with 30% probability ellipsoids. Selected bond lengths (Å): Ru1–Re1 = 2.5261(3), Re1–P1 = 2.3622(10), Re1–P2 = 2.2895(10), Re1–P3 = 2.3749(12).

from cold pentane and cold heptane, respectively. The ORTEP diagrams are shown in Figures 5 and 6, respectively. Complex **6** reveals a binuclear structure having both Ru and Re. The Ru–Re bond is triply bridged by hydrogen atoms, and two hydrogen atoms are located at the terminal sites of the Re atom. The coordination geometries at Ru and Re are described as a three-legged piano stool and a pseudo pentagonal bipyramidal, respectively, in which the centroid of the Cp' group and H1 occupy the axial positions and the H2, H3, H4, and H5 atoms are on the equatorial plane.

Complex **9** has a binuclear structure linked by three hydrogen atoms. A hydrogen atom is bound to the Re atom as a terminal hydride. Three phosphorus atoms bound to the rhenium center occupy a *cis* position and two *trans* positions with respect to the terminal hydride. The geometries at Ru and Re are a three-legged piano stool and a pseudo capped octahedron, respectively.

The Ru–Re distances of **6** and **9** are 2.4798(5) and 2.5261(3) Å, respectively. These short Ru–Re distances indicate a multiple metal–metal bond.²⁰ The 18-electron rule dictates that there be a metal–metal triple bond. The distances are slightly shorter than those of the isoelectronic dinuclear complexes (CO)(PMePh₂)₂–Re(μ -H)₃Ru(PPh₃)₃ (Ru–Re = 2.595(1) Å)^{4b} and (CO)(PPh₃)₂–(H)Re(μ -H)₃Ru(H)(PPh₃)₂ (Ru–Re = 2.593(2) Å)^{4c} and

the 32-electron complex (CO)(PPh₃)₂Re(μ -H)₂(μ -NCHPh)Ru(PHCN)(PPh₃)₂ (Ru–Re = 2.654(1) Å).^{4d} The Ru–Re bond is shortened by substitution of the phosphine ligand with the strongly electron-releasing Cp' ligand, and the coordination of the electron-withdrawing CO ligand leads to elongation of the Ru–Re bond.

Synthesis of Heterotrimetallic Polyhydride Complexes. An increase in the nuclearity of the cluster complex possibly enhances its capability for multiple coordination and multielectron transfer. In the synthesis of a trinuclear complex consisting of an Ru₂Re framework, our first attempt failed. The reaction of Cp'ReH₆ (**2**) with an equimolar amount of (Cp'Ru)₂(μ -H)₄ (**1**) proceeded nonselectively to result in the formation of a mixture of **6**, (Cp'Ru)₂(Cp'Re)(μ -H)₄ (**7**), and (Cp'Ru)(Cp'Re)₂(H)₅ (**8**) in a ratio of 72:1:27, respectively. Distribution of the products **6**–**8** is hardly affected by the molar ratio of the starting materials. In the reaction of Cp'ReH₆ with 2 mol of (Cp'Ru)₂(μ -H)₄, the product ratio **6**:**7**:**8** changed to 72:2:25. In addition, although the dinuclear complex **6** was isolated by column chromatography, trinuclear complexes **7** and **8** were inseparable in a pure form, unfortunately. Therefore, this method is not appropriate for the synthesis of trinuclear complexes with an Ru₂Re or RuRe₂ framework.

As reported previously, we had prepared the cationic trinuclear complex of ruthenium [(Cp'Ru)₃(μ -H)₃]X by the reaction of (Cp'Ru)₂(μ -H)₄ with an acid HX such as HBF₄ or CF₃SO₃H in diethyl ether.²¹ We applied this method to the synthesis of a new heterotrimetallic cluster having an Ru₂Re core.

Reaction of **6** with 1/2 mol of HBF₄ in diethyl ether smoothly proceeded at room temperature to lead to the exclusive formation of the cationic trinuclear complex [(Cp'Ru)₂(Cp'Re)(μ -H)₅][BF₄] (**10a**), together with the mononuclear rhenium hexahydride **2** (Scheme 3). Complex **10a** is the first example of a mixed-metal polyhydride complex with a triangular Ru₂Re core that has no auxiliary ligands other than C₅Me₅ groups. Complex **10a** readily undergoes an exchange of a counteranion by treatment with excess NaBPh₄ to give [(Cp'Ru)₂(Cp'Re)(μ -H)₅][BPh₄] (**10b**).

Complexes **10a** and **10b** were unambiguously identified by NMR spectroscopy as well as X-ray diffraction studies. The ¹H NMR spectrum of **10a** measured at room temperature in acetone-*d*₆ exhibited two singlet signals of the Cp' group at δ 2.32 (15 H) and 1.97 (30 H). The former was ascribed to the Cp' group coordinated to the rhenium atom. The signals of the hydrides were observed at δ –9.52 and –11.31 in the intensity ratio 1:4 at room temperature. The ¹H NMR spectrum shows that complex **10a** has a symmetry plane bisecting the Ru₂Re isosceles triangle. Therefore, we tentatively assigned the signals at δ –9.52 and –11.31 as the hydride bridging the two ruthenium atoms and that bridging the ruthenium and the rhenium, respectively. The fluxionality of the hydride ligands in the cationic complex **10** was examined by means of VT ¹H NMR spectroscopy using **10b** as a probe compound (Figure 7). Although the two sharp singlet signals of the

(20) Cotton, F. A.; Walton, R. A. In *Multiple Bonds between Metal Atoms*, 2nd ed.; Oxford University Press: New York, 1993; Chapters 2 and 9.

(21) (a) Suzuki, H. *Eur. J. Inorg. Chem.* **2002**, 1009. (b) Suzuki, H.; Kakigano, T.; Tada, K.; Igarashi, M.; Matsubara, K.; Inagaki, A.; Ohshima, M.; Tanaka, M. Unpublished results.

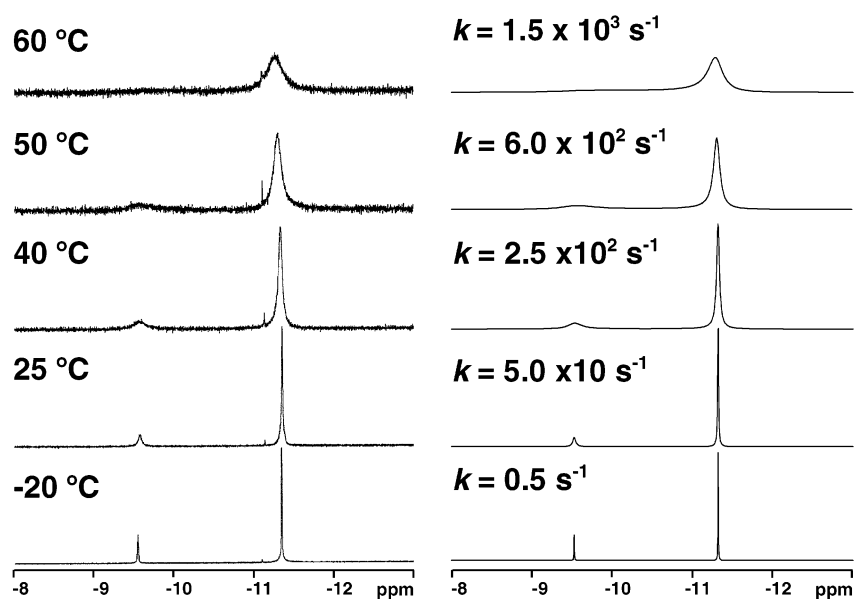
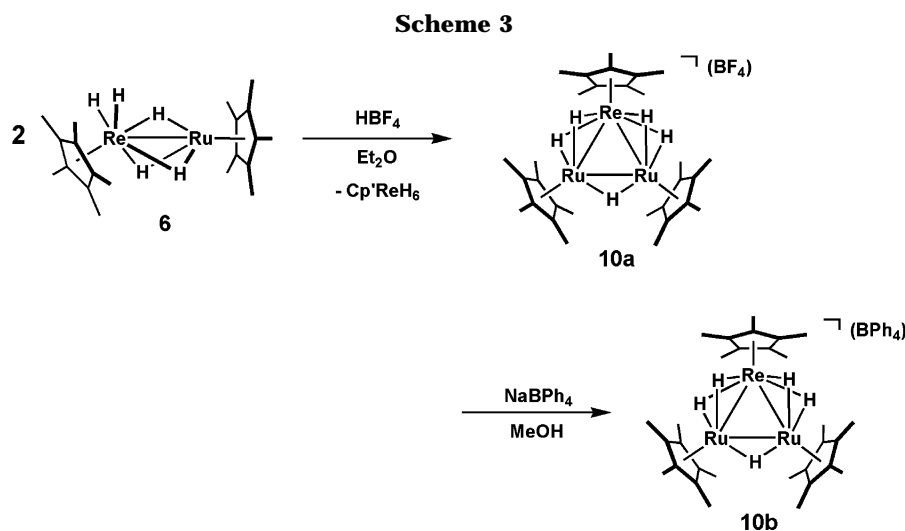
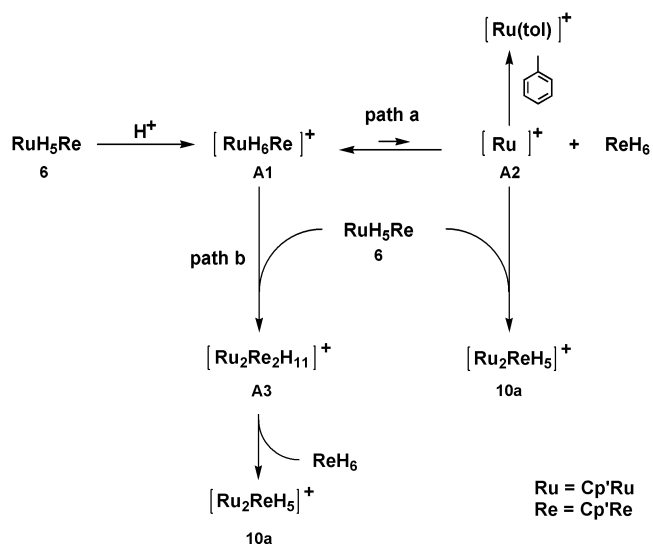


Figure 7. Experimental (left) and simulated (right) variable-temperature ^1H NMR spectra of **10b** showing the region of the hydride protons.



Scheme 4



hydrides gradually broadened with an increase in the temperature, they did not coalesce into one peak, even at 60 °C. As a result of the line-shape analysis, the activation parameters for the site exchange among the bridging hydrides were estimated to be $\Delta H^\ddagger = 16.1(5)$ kcal mol $^{-1}$ and $\Delta S^\ddagger = 3.7(17)$ cal mol $^{-1}$ K $^{-1}$.

For the formation of the trinuclear complex **10a**, we propose the following two reaction paths (Scheme 4). One is a *coupling pathway*, which involves the coupling of **6** with the highly unsaturated 12e species $[\text{Cp}'\text{Ru}]^+$, formed as a result of fragmentation of a protonated product of **6**, $[\text{Cp}'\text{RuH}_6\text{ReCp}']^+$ (**A1**) (path a). The other is a *fragmentation pathway*, which involves fragmentation of $\text{Cp}'\text{ReH}_6$ from the cationic tetranuclear complex $[(\text{Cp}'\text{Ru})_2(\text{Cp}'\text{Re})_2\text{H}_{11}]^+$ (**A3**), formed via a coupling of **6** with $[\text{Cp}'\text{RuH}_6\text{ReCp}']^+$ (**A1**) (path b).

To distinguish between these two reaction pathways, the controlled reactions were examined by monitoring the product formation or disappearance of the starting material over time. To a tetrahydrofuran-*d*₈ solution of **6** with a concentration of 2.3×10^{-2} M was added 11 equiv of HBF_4 , and the reaction was monitored by means

of ^1H NMR spectroscopy at -80 °C (Figure 8). The reaction proceeded even at -80 °C, and the ^1H NMR spec-

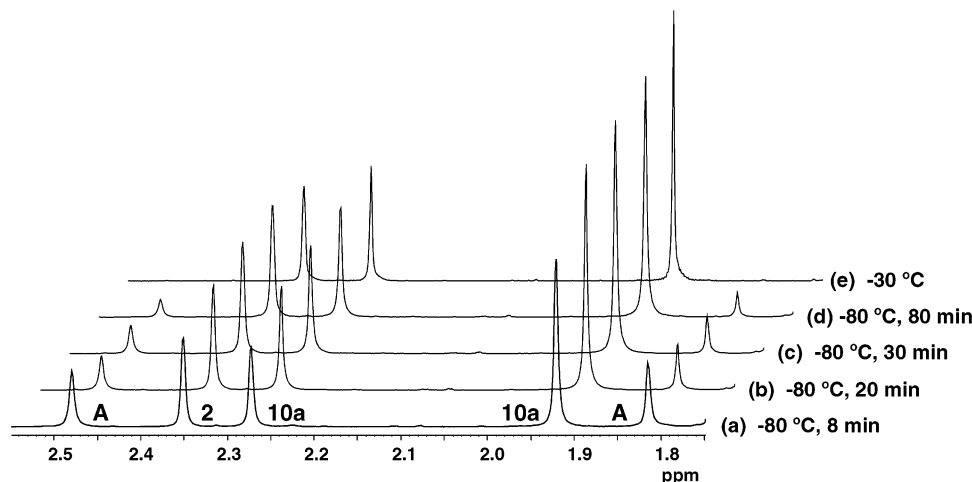


Figure 8. ^1H NMR spectra of the reaction of **6** with HBF_4 showing the region of the Cp' methyl protons.

trum (Figure 8a) showed that the starting complex **6** was consumed in the reaction and the Cp' signals of **6** at δ 1.84 and 2.14 almost disappeared after 8 min. At this stage, the formation of **10a**, Cp'ReH₆, and the unidentified product **A** was observed. The molar ratio of **10a** and Cp'ReH₆ was 1:1, on the basis of the integral intensity of the Cp' signals. The unidentified product **A** revealed two singlet signals for Cp' ligands at δ 1.82 and 2.48 ppm and a broad signal for the hydrides at δ -8.63 ppm in the intensity ratio 30:30:11, respectively. The sum of the intensities of the Cp' signals of **A** was less than 20% of that of the starting complex **6**. With the elapse of time (Figure 8b–d), **A** was converted to **10a** and Cp'ReH₆. The signals of **A** disappeared at -30 °C, and no signals other than those of **10a** and Cp'ReH₆ were observed in the ^1H NMR spectrum (Figure 8e). The molar ratio of the products, **10a** and Cp'ReH₆, was 1:1, and it remained unchanged throughout the reaction. These results show that **A** was the intermediary tetranuclear complex $[(\text{Cp}'\text{Ru})_2(\text{Cp}'\text{Re})_2\text{H}_{11}]^+$, which was converted to a 1:1 mixture of cationic trinuclear cluster **10a** and mononuclear rhenium hydride complex Cp'ReH₆. The presence of no intermediate other than $[(\text{Cp}'\text{Ru})_2(\text{Cp}'\text{Re})_2\text{H}_{11}]^+$ and the constancy of the product distribution, **10a**:Cp'ReH₆ = 1:1, throughout the reaction strongly indicate that **10a** and Cp'ReH₆ are formed by way of fragmentation of the cationic tetranuclear undecahydride $[(\text{Cp}'\text{Ru})_2(\text{Cp}'\text{Re})_2\text{H}_{11}]^+$ (**A**), generated as a result of coupling between **10a** and $[\text{Cp}'\text{ReH}_6\text{RuCp}']^+$.

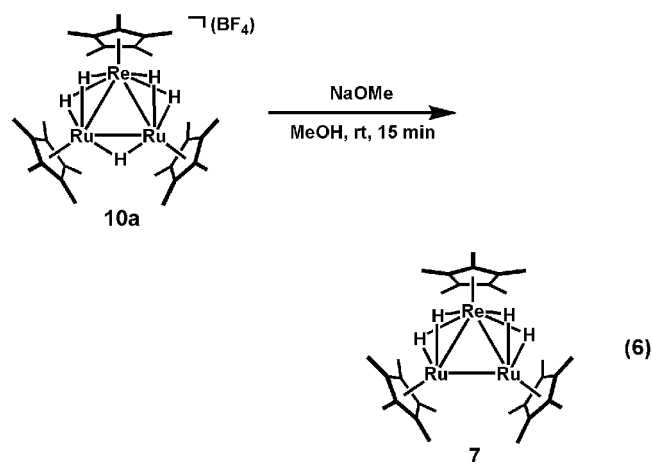
However, we cannot disregard the possibility of path a, which involves coupling of **6** with the highly unsaturated 12e species $[\text{Cp}'\text{Ru}]^+$, formed as a result of fragmentation of a protonated product of **6**, $[\text{Cp}'\text{RuH}_6\text{ReCp}']^+$. We examined the reaction of **6** with HBF_4 in the presence of a 6e donor ligand to capture the 12e species $[\text{Cp}'\text{Ru}]^+$. Previously, we reported that $[\text{Cp}'\text{Ru}]^+$ formed in the reaction of $\text{Cp}'\text{Ru}(\mu\text{-H})_4\text{RuCp}'$ (**1**) with protic acid in diethyl ether was readily captured by $\text{C}_6\text{H}_5\text{R}$ (R = H, CH₃) to yield the saturated cationic arene complex $[\text{Cp}'\text{Ru}(\text{C}_6\text{H}_5\text{R})]^+$ selectively.^{1a} If the unsaturated species $[\text{Cp}'\text{Ru}]^+$ is generated in the reaction of **6** with HBF_4 according to path a in the presence of a 6e donor ligand such as arene, it should be trapped to form the saturated species.

The reaction of **6** with 1 equiv of $\text{HBF}_4(\text{OMe}_2)$ in toluene led to the formation of **10a**, Cp'ReH₆, and

$[\text{Cp}'\text{Ru}(\eta^6\text{-C}_6\text{H}_5\text{CH}_3)](\text{BF}_4)$ together with two unidentified minor products. The amount of unidentified products was estimated to be less than 20%, on the basis of the integral intensity of Cp' signals. The molar ratio among **10a**, Cp'ReH₆, and $[\text{Cp}'\text{Ru}(\eta^6\text{-C}_6\text{H}_5\text{CH}_3)](\text{BF}_4)$ was 1.0:0.74:0.05, respectively. It should be noted that the reaction was conducted in a dilute solution (8.5×10^{-3} M) of **6** in toluene. Although the molar ratio of toluene to complex **6** in the reaction system is more than 1000, the product ratio between $[\text{Cp}'\text{Ru}(\text{C}_6\text{H}_5\text{CH}_3)](\text{BF}_4)$ and **10a** was 1:20. Since coordinative addition of $\text{C}_6\text{H}_5\text{CH}_3$ to the highly unsaturated species $[\text{Cp}'\text{Ru}]^+$ is a very rapid process, this result strongly implied that fragmentation of the bimetallic cation $[\text{Cp}'\text{ReH}_6\text{RuCp}']^+$ into Cp'ReH₆ and $[\text{Cp}'\text{Ru}]^+$ is a relatively slow and minor process for the formation of **10a**. We therefore concluded that **10a** was produced mainly by way of path b.

Electron density at the metal centers of a neutral cluster is likely higher than that of a cationic cluster. The neutral cluster is, therefore, much more active than cationic clusters in reactions in which an oxidative addition process is involved. Thus, we performed deprotonation of cationic complex **10a** to obtain the neutral complex **7**.

Treatment of **10a** with NaOMe in MeOH afforded the neutral trinuclear cluster $(\text{Cp}'\text{Ru})_2(\text{Cp}'\text{Re})(\mu\text{-H})_4$ (**7**) in 90% yield (eq 6). We similarly synthesized $(\text{C}_5\text{Me}_4\text{EtRu})_2(\text{Cp}'\text{Re})(\mu\text{-H})_4$ (**7'**) by starting from **6'**.



The ^1H and ^{13}C NMR spectra clearly showed that

these complexes had a core consisting of two ruthenium atoms and a rhenium atom.

In the ^1H NMR spectrum of **7** measured in C_6D_6 , two singlet peaks were observed at δ 2.14 (15 H) and 1.91 (30 H). As mentioned below, they were assigned as the signals of Cp' groups bound to the rhenium and the ruthenium centers, respectively, by comparison with the ^1H NMR spectrum of $(\text{C}_5\text{EtMe}_4\text{Ru})_2(\text{Cp}'\text{Re})(\mu\text{-H})_4$ (**7'**).

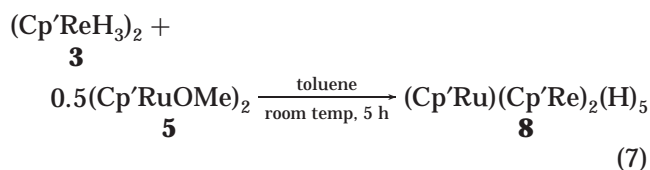
The ^1H NMR spectrum of **7'** revealed a Cp' signal bound to rhenium at δ 2.15 (15H) and a set of signals of the $\text{C}_5\text{Me}_4\text{Et}$ group bound to ruthenium at δ 1.94 (s, 12H), 1.92 (s, 12H), 2.51 (q, 4H), and 1.09 (t, 6H). Thus, the chemical shift of δ 2.14 and 1.91 observed in the ^1H NMR spectrum of **7** could be assigned to the Cp' groups bound to rhenium and ruthenium, respectively. On the basis of the integral intensities of these signals, we conclude that both **7** and **7'** had an Ru_2Re core.

In both the ^1H and ^{13}C NMR spectra of **7** and **7'**, the signals of the $\text{C}_5\text{Me}_4\text{R}$ ligand (**7**, R = Me; **7'**, R = Et) on the ruthenium centers were observed to be equivalent, and the resonance signal for the hydride appeared at δ -13.71 as a singlet with an intensity of 4H. These results indicated the presence of a pseudo-symmetry element passing through the rhenium center and the midpoint of the two ruthenium atoms. Accordingly, we tentatively concluded that each of the two Ru–Re edges of the Ru_2Re core was doubly bridged by the hydride. This assignment of the location of the hydride ligands was supported by the fact that the line shape of the ^1H signal for the hydride ligands remained almost unchanged, even at -80°C .

As mentioned above, a heterotrimetallic cluster with a different combination of the metals, $(\text{Cp}'\text{Ru})(\text{Cp}'\text{Re})_2(\text{H})_5$ (**8**), was formed in the reaction of $\text{Cp}'\text{ReH}_6$ (**2**) with $\text{Cp}'\text{Ru}(\mu\text{-H})_4\text{RuCp}'$ (**1**) as a minor product. However, we could not obtain **8** in a pure form, unfortunately. We attempted alternative methods by way of dehydrogenative coupling, such as the reaction of **1** with dirhenium hexahydride $(\text{Cp}'\text{ReH}_3)_2$ (**3**), to obtain **8** in high yield. Although we could obtain **8** in some reactions, all the results were unsatisfactory.

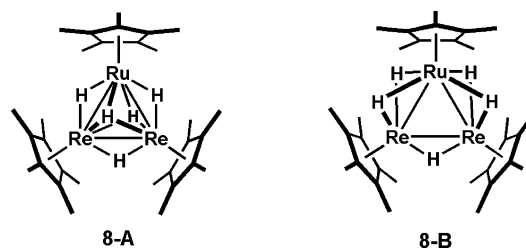
We have already reported that a dinuclear methoxo complex of ruthenium, $(\text{Cp}'\text{Ru})_2(\mu\text{-OMe})_2$ (**5**), is a versatile precursor for the synthesis of heterometallic clusters such as $\text{Cp}'\text{Ru}(\mu\text{-H})_3\text{IrCp}'$.^{5a} The methoxo complex **5** is used as a synthetic equivalent of the "Cp'Ru" fragment in the synthesis of the heterometallic cluster. We followed the precedent and adopted **5** and dirhenium hexahydride $(\text{Cp}'\text{ReH}_3)_2$ (**3**) as the precursors of the "Cp'Ru" and "(Cp'Re)₂" fragments, respectively.

The reaction of **5** with 2 mol of **3** readily proceeded in toluene, even at ambient temperature, to give **8** selectively (eq 7). It is noteworthy that the rhenium–rhenium bond is strong enough not to be cleaved and neither **6** nor **7** is formed in this reaction.



In a similar manner, $(\text{C}_5\text{Me}_4\text{EtRu})(\text{Cp}'\text{Re})_2(\text{H})_5$ (**8'**) was prepared by the reaction of $(\text{C}_5\text{Me}_4\text{EtRu})_2(\mu\text{-OMe})_2$

Chart 1



(**5'**) with **3**. Complex **8** is a highly air- and moisture-sensitive black solid and is soluble in a wide range of solvents, such as benzene, toluene, pentane, ether, and methanol.

The ^1H NMR spectrum of **8** revealed three singlet signals at δ 2.29 (30 H), 1.73 (15 H), and -12.67 (5H). On the basis of the intensity and chemical shift of the signals, they were assigned to the Cp' groups bound to the rhenium, the ruthenium, and the hydride ligands, respectively. The assignment of two Cp' signals was fully consistent with that of **8'**, in which the Cp' group on the ruthenium atom was substituted with $\text{C}_5\text{Me}_4\text{Et}$. The signal of the Cp' group on the rhenium was observed at δ 2.29 (30 H), and a set of signals of the $\text{C}_5\text{Me}_4\text{Et}$ ligand appeared at δ 1.76 (s), 1.73 (s), 2.35 (q), and 0.99 (t) in an intensity ratio of 6H:6H:2H:3H.

The number of hydride ligands was confirmed to be 5, on the basis of the intermolecular H/D exchange reaction between the hydrides and C_6D_6 , which likely proceeded via oxidative addition of C_6D_6 to **8** followed by reductive elimination of $\text{C}_6\text{D}_5\text{H}$. The H/D exchange reaction was monitored by means of ^1H NMR spectroscopy. Upon heating of **8** in C_6D_6 to 80°C , the signals of the hydrides of isotopomers formed as a result of the H/D exchange reaction were observed at δ -12.67 (**8-d₀**), -12.71 (**8-d**), -12.74 (**8-d₂**), -12.77 (**8-d₃**), and -12.81 (**8-d₄**). Although the intensities of the signals of the isotopomers with higher molecular weight increased with the elapse of time, no signal other than those of the aforementioned five isotopomers appeared. This evidently shows that **8** has five hydride ligands in the molecule.

The ^1H and ^{13}C NMR spectra of **8**, which reveal two Cp' signals with an intensity ratio of 1:2 in the temperature range from $+25$ to -80°C imply that **8** has a symmetry element, namely, a symmetry axis or plane, through the ruthenium atom and the midpoint between the two rhenium atoms. Chart 1 exhibits the plausible location of the hydride ligands in **8-A** and **8-B**. **8-A** has triply bridged hydrides capped at the Ru_2Re plane, and **8-B** has only doubly bridged hydrides at the Ru–Ru and Ru–Re edges. Both **8-A** and **8-B** have symmetrical structures, which are consistent with the NMR spectral data mentioned above. Despite the nonequivalency of the magnetic environments of the hydride ligands, they were observed to be equivalent at δ -12.67 at room temperature. This is most likely due to rapid exchange of the coordination sites of the hydride. A decrease in temperature causes a slowdown of the exchange process. As a result, a significant broadening of the signal was observed at low temperature ($w_{1/2} = 66$ Hz at -80°C). We could not, unfortunately, pinpoint the location of the hydride ligands, because the resonance signal did not split even at low temperature.

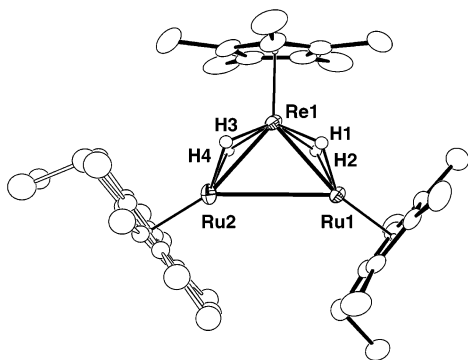


Figure 9. ORTEP diagram of the solid-state molecular structure of **7'** with 50% probability ellipsoids. Selected bond lengths (Å): Ru1–Re1 = 2.5149(11), Ru2–Re1 = 2.5103(8), Ru1–Ru2 = 3.2334(11).

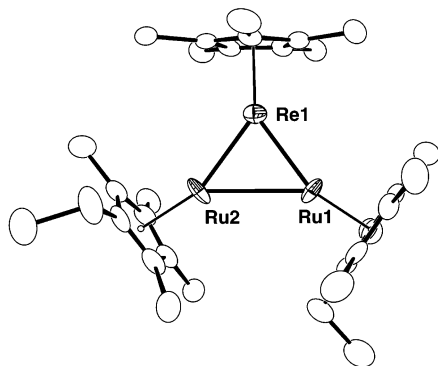


Figure 10. ORTEP diagram of the solid-state molecular structure of **10b'** with 50% probability ellipsoids. Selected distances (Å): Re1–Ru1 = 2.5304(14), Re1–Ru2 = 2.5506(14), Ru1–Ru2 = 2.9297(16).

Structures of the Trimetallic Complexes. Complex **7** has three C_5Me_5 ligands on each metal center. In such cases, the molecular structure is often disordered, despite the unsymmetrical metal core. To avoid the disordered arrangement of the three metal atoms, a structure determination of the trimetallic complex **7** was performed by using **7'**, which has a C_5Me_5 ligand on the rhenium atom and a C_5Me_4Et ligand on the ruthenium atoms. The molecular structure of **7'** is shown in Figure 9. There is rotational disorder at the C_5Me_4Et ligand at the Ru2 center. The Ru_2Re core is an approximate isosceles triangle. The Ru and Re atoms are doubly bridged by hydrogen atoms, and the Ru–Re distances are 2.5103(8) and 2.5149(11) Å. These values are comparable to those of **6** and **9**. No hydrogen atoms are located between the two ruthenium atoms. The Ru–Ru distance of 3.2334(11) Å is considerably longer than that of the Ru–Ru single bond reported thus far. If each ruthenium atom adopts a three-legged piano-stool geometry, there should be a bonding interaction between the two ruthenium atoms.

To avoid the disordered arrangement of the three metal centers, we performed a structure determination using $[(C_5EtMe_4Ru)_2(Cp/Re)(\mu-H)_5][BPh_4]$ (**10b'**). The BPh_4 anion is omitted for clarity. As observed in the neutral complex **7'**, there is an isosceles triangular Ru_2Re core with one long Ru–Ru bond and two short Ru–Re bonds. The Ru–Re bonds of 2.5304(14) and 2.5506(14) Å are slightly longer than that of **7'**. On the

other hand, the Ru–Ru distance of 2.9297(16) Å is shorter than that observed in **7'**. Although the hydrogen atoms directly bound to the metal atoms were not located in the Fourier maps, they could be positioned on the basis of the metal–metal distances as well as the 1H NMR spectral data of **10b**. It is reasonable to conclude that the Ru and the Re atoms are doubly linked with a hydrogen atom and a hydrogen atom bridges the two ruthenium atoms. The Ru–Re and Ru–Ru distances of about 2.5 and 2.9 Å, respectively, are quite consistent with the proposed locations of the hydrogen atoms.

H/D Exchange Reaction between the Heterotrimetallic Complexes and D_2 or C_6D_6 . We have proved that the hydride ligands in the heterobimetallic complex **9** underwent H/D exchange with D_2 and C_6D_6 . The capability of interaction between the two hydride ligands to form an intermediary η^2-H_2 complex is likely crucial to the exchange reaction. Coordination of D_2 or C_6D_6 to the vacant site, generated as a result of a bonding interaction between the two hydride ligands, would lead to oxidative addition of a D–D or an aromatic C–D bond, respectively. As mentioned above, the intermolecular H/D exchange reaction is characteristic of the polyhydride complex. Thus, we examined the reaction of a heterometallic cluster with higher nuclearity with D_2 or C_6D_6 . While the dinuclear complex **6** undergoes H/D exchange with neither D_2 nor C_6D_6 , the trinuclear complexes **7** and **8** are much more active in the exchange reaction. The reaction of **7** with D_2 in $THF-d_8$ was monitored by means of 1H NMR spectroscopy at room temperature. The reaction of **7** with D_2 proceeded along two independent paths: namely, one path leading to a paramagnetic species and the other to intermolecular H/D exchange. With the passage of time, the intensity of the resonance signal of the hydrides decreased due to both H/D exchange with D_2 and conversion into the paramagnetic species, for which broad signals were observed at δ 17.77 ($w_{1/2}$ = 1100 Hz) and 12.59 ($w_{1/2}$ = 370 Hz) in the 1H NMR spectrum with an intensity ratio of 2:1. As a result of the H/D exchange reaction, signals of the isotopomers **7-d**, **7-d₂**, **7-d₃**, and **7-d₄** appeared in the hydride region. After 45 h, conversion of **7** to the paramagnetic species reached nearly 60%, and the rest consisted of a 5:25:70 mixture of the isotopomers **7-d₂**, **7-d₃**, and **7-d₄**. At this point, 91% of the hydride ligands in the remaining **7** were exchanged with deuterides.

Complex **8** also underwent H/D exchange under atmospheric pressure of D_2 , and the rate of the H/D exchange for **8** was comparable to that for **7**. Notably, in the reaction of **8** under atmospheric pressure of D_2 at room temperature, no products other than isotopomers **8-d_n** (n = 0–5) were observed. Upon exposure to D_2 for 45 h at room temperature, 92% of the hydride ligands in **8** were substituted with deuterium and the isotopomer ratio **8-d₀**:**8-d₁**:**8-d₂**:**8-d₃**:**8-d₄**:**8-d₅** reached 0:0:0:7:23:70. In contrast, the H/D exchange reaction of cationic complex **10a** with D_2 proceeded much more slowly than those of **7** and **8**, probably due to low electron density at the metal centers of **10a**. As a result, oxidative addition of D_2 is likely retarded in **10a** in comparison with **7** and **8**. As cluster **10a** is a coordinatively unsaturated 42e complex, coordination of D_2 would, therefore, proceed via an associative path to

generate the intermediate $[(\text{Cp}'\text{Ru})_2(\text{Cp}'\text{Re})(\mu\text{-H})_3(\eta^2\text{-H}_2)(\eta^2\text{-D}_2)]^+$, which undergoes oxidative addition of D_2 and subsequent reductive elimination of HD to form the isotopomer $[(\text{Cp}'\text{Ru})_2(\text{Cp}'\text{Re})(\mu\text{-H})_4(\mu\text{-D})]^+$ (**10a-d**). The D_2 molecule is small enough to enter freely into the reaction field surrounded by the three Cp' ligands. Therefore, it is reasonable to assume that the rate-determining step of the H/D exchange with D_2 is oxidative addition rather than the coordination of D_2 .

H/D exchange also occurs between the heterotrimeric polyhydride complexes and C_6D_6 . However, the rate of exchange with C_6D_6 is much slower than that with D_2 . In C_6D_6 , it took about 210 h to substitute 30% of the hydride in **7** for deuterium, while the conversion of the H/D exchange reached 30% after 3 h in the reaction with D_2 . Similarly, it took about 270 h to substitute 40% of the hydride for deuterium in the reaction of **8** with C_6D_6 . This is probably due to the difference in the rate-determining step for the H/D exchange with C_6D_6 and that with D_2 . The molecular size of C_6D_6 is much larger than that of D_2 . Therefore, we propose that the rate-determining step of the H/D exchange with C_6D_6 is most probably the step of capture of C_6D_6 in the triangular space surrounded by the three Cp' groups. We previously showed on the basis of a kinetic study that capture of the substrate in the triangular reaction field was the rate-determining step in the reaction of $(\text{Cp}'\text{Ru})_3(\mu\text{-H})_3(\mu_3\text{-H})_2$ with 1,3-cyclohexadiene.²² This result is consistent with our proposal.

In summary, the synthesis and structure determination of several new bi- and trinuclear polyhydride complexes containing ruthenium and rhenium were performed. Those polyhydride complexes were unprecedented types of clusters containing Cp' and triphos groups as ancillary ligands. The reaction of **6** with HBF_4

led to the selective formation of cationic trinuclear complex **10a** and $\text{Cp}'\text{ReH}_6$ in a ratio of 1:1. Monitoring the reaction by means of ^1H NMR spectroscopy revealed that **10a** was formed via fragmentation of the tetranuclear intermediate $[(\text{Cp}'\text{Ru})_2(\text{Cp}'\text{Re})_2\text{H}_{11}]^+$, formed as a result of coupling of **6** with the protonated binuclear complex $[\text{Cp}'\text{RuH}_6\text{ReCp}']^+$. The hydride ligands of **6-9** and **10a** underwent both an intramolecular exchange of the coordination sites and an intermolecular H/D exchange with D_2 or C_6D_6 . The activation parameters for the site exchange of the hydride ligands between the terminal and bridging sites of **6** and **9** were estimated by simulation of the variable-temperature ^1H NMR spectra. As expected for **9**, introduction of a flexible triphos ligand to the cluster framework enhanced the mobility of the hydride ligands. The H/D exchange reaction of trinuclear complexes **7** and **8** with D_2 was faster than those of binuclear complexes **6** and **9**. The H/D exchange reaction of hydrides in **7** and **8** with C_6D_6 was a slow process in comparison to that with D_2 , because of the bulkiness of the C_6D_6 molecule relative to the size of the reaction field.

Acknowledgment. We appreciate financial support from the Ministry of Education, Culture, Sports, Science and Technology of Japan (Grant Nos. 15205009 and 14078210 "Reaction Control of Dynamic Complexes"). This work was partly supported by The 21st Century COE Program. We also acknowledge Kanto Chemical Co., Inc., for generous gifts of pentamethylcyclopentadiene.

Supporting Information Available: Text giving details of the simulation for the VT ^1H NMR studies of **6**, **9**, and **10b**, tables and plots of the H/D exchange reaction of **7**, **8**, **9**, and **10b'**, and X-ray crystallographic data of **6**, **7'**, **9**, and **10b'** in CIF form. This material is available free of charge via the Internet at <http://pubs.acs.org>.

OM030651E

(22) Inagaki, A.; Takaya, Y.; Takemori, T.; Suzuki, H. *J. Am. Chem. Soc.* **1997**, *119*, 625.